II.B Energy-Efficient Emission Controls

II.B.1 Fundamental Studies of NOx Adsorber Materials

Rob Disselkamp, Do Heui Kim, Ja Hun Kwak, Janos Szanyi, Tamas Szailer, Russ Tonkyn, and Chuck Peden (Primary Contact)
Pacific Northwest National Laboratory
P.O. Box 999, MS K8-93
Richland, WA 99352

DOE Technology Development Manager: Ken Howden

Objectives

- Develop a practical fundamental understanding of NOx adsorber technology operation.
- Focus on chemical reaction mechanisms correlated with catalyst material characterization.
- Interact with Oak Ridge National Laboratory (ORNL) project aimed at development of 'aging' protocols (Bruce Bunting) and with Lawrence Livermore National Laboratory (LLNL) modeling effort (Chris Mundy and Bill Pitts). Actively participate in the Cross-Cut Lean Exhaust Emission Reduction Simulation (CLEERS) lean-NOx trap (LNT) subgroup. This now includes an additional 3-way collaboration between ORNL (Stuart Daw and coworkers), Sandia National Laboratories (SNL) (Rich Larson), and Pacific Northwest National Laboratory (PNNL).
- Transfer the developing fundamental understanding to industry via the CLEERS activity as well as periodic technical meetings with industry scientists and engineers.

Approach

- Utilize state-of-the-art catalyst characterization and testing facilities in the Institute for Interfacial Catalysis at PNNL, including:
  - Synchrotron temperature-programmed X-ray diffraction (XRD): catalyst structural changes
  - Transmission electron microscopy/energy dispersive X-ray (TEM/EDX) and scanning electron microscopy (SEM): catalyst morphological changes
  - X-ray photoelectron spectroscopy: oxidation state and relative surface concentrations
  - Fourier transform infrared (FTIR) and nuclear magnetic resonance (NMR) spectroscopies: catalyst reaction mechanisms
  - Temperature-programmed desorption/thermal gravimetric analysis (TPD/TGA): surface chemistry
  - Lab reactor: performance measurements, kinetics and mechanisms
- Hold periodic review meetings open to all interested industry scientific and engineering staff. First one of these was held in Detroit, October 19, 2004. Participate as an active member of the CLEERS subgroup on LNTs.

Accomplishments

- Constructed a laboratory reactor for measurements of transient lean-rich cycling performance for LNT catalyst monolith cores – includes special capability for 'nitrogen-balance' experiments.
- Spectroscopic identification of two morphological 'forms' of the storage Ba-phase – a 'monolayer' phase and a 'bulk' phase. Directly observed dynamic morphology changes as a function of NOx uptake and

release by *in-situ* temperature-programmed x-ray diffraction (TP-XRD), and *ex-situ* with transmission electron microscopy with elemental analysis by energy dispersive spectroscopy (TEM/EDS).

- Reactivity studies of model LNT materials with varying Ba loadings suggest an optimum storage material morphology.
- Significant effects of LNT preparation methods and LNT and support composition were observed and led to two new invention disclosures.
- Initiated experiments and modeling of NO oxidation reaction.
- Measured nitrogen 'speciation' in the products formed during rich regeneration, and able to obtain a good 'nitrogen balance' in these experiments.
- Numerous publications, invited talks, and other presentations have resulted from this project (see list of reports).

Future Directions

- BaO morphology studies.
  - Effects of CO_2 and/or H_2O on morphology changes during NOx uptake and release. TP-XRD studies to be performed at the National Synchrotron Light Source as beamtime becomes available.
  - *In-situ* TEM studies to watch morphology changes in real time.
  - Effects of additional catalyst components (e.g., ceria as used in CLEERS Umicore material) and alternative support materials (e.g., MgO and $MgAl_2O_4$).
  - Role of Pt/BaO interface for optimum NOx storage.
- Detailed characterization (e.g., FTIR, TEM) of alternative materials.
- NO oxidation reaction – Pt particle size dependence.
- Studies of CLEERS Umicore samples.
  - CLEERS performance protocol experiments.
  - Nitrogen balance experiments (mechanism(s) of reductive regeneration).

Introduction

One of the key challenges facing the catalysis community is the elimination of harmful gases emitted by internal combustion engines. In particular, the reduction of NOx from an exhaust gas mixture that contains an excess amount of oxygen is difficult. Traditional three-way catalysts do not work under lean conditions because the concentrations of the reductants (CO and hydrocarbons) are greatly reduced by their oxidation with O_2 on the noble metal components of these catalysts. Therefore, new approaches to NOx reduction have been considered in the last decade. In spite of all the efforts to develop new emission control technologies for lean NOx reduction, only limited applications have been achieved. One of the most promising technologies under consideration is the NOx adsorber catalyst (aka NOx storage/reduction, NSR, or lean NOx trap, LNT) method. This process is based on the ability of certain oxides, in particular alkaline and alkaline earth oxide materials, to store NOx under lean conditions and release it during rich (excess reductant) engine operation cycles. Since the original reports on this technology from Toyota in the mid `90s [1], the most extensively studied catalyst system continues to be based on barium oxide (BaO) supported on a high-surface-area alumina (Al_2O_3) material [2].

Our project is aimed at developing a practically useful fundamental understanding of the operation of the LNT technology, especially with respect to the optimum materials used in LNTs. As noted above in the summary Accomplishments section, we have made significant progress in a fairly wide array of areas. For the purposes of this report, we briefly highlight progress in two areas: i) the identification of several specific morphologies for Ba-phases on alumina and how these morphologies change as a

function of NOx loading to form $Ba(NO_3)_2$ and its subsequent thermal decomposition; and ii) the time-resolved measurement of all nitrogen-containing products, including N_2, during lean-rich cycling experiments on a commercial (Umicore) LNT material.

Experimental Details

Catalyst Preparation and Characterization.

The BaO/Al_2O_3 NSR catalysts were prepared by the incipient wetness method, using an aqueous $Ba(NO_3)_2$ solution (Aldrich) and α-alumina support (200 m^2/g, Condea) to yield nominal 2, 8 and 20 wt% BaO-containing samples, dried at 125°C and then 'activated' via a calcination at 500°C in flowing dry air for 2 h. State-of-the-art techniques such as XRD, X-ray photoelectron spectroscopy (XPS), TEM/EDS, FTIR, BET (Brunauer-Emmet-Teller)/pore size distribution, and temperature-programmed desorption/reaction (TPD/TPRX), available at PNNL, were utilized to probe the changes in physicochemical properties of the catalyst samples. The time-resolved X-ray diffraction (TR-XRD) experiments were carried out at beam line X7B of the National Synchrotron Light Source at Brookhaven National Laboratory. The detailed experimental set-up and protocol have been discussed elsewhere [3,4].

Reactor and Procedures for Nitrogen Balance Experiments.

We completed construction of a new experimental apparatus for conducting the nitrogen balance experiments. *As far as we know, our studies represent the only quantitative measurement of nitrogen balance for LNT operation conducted to date.* The apparatus we built, briefly described here and in more detail in [5], contains a gas handling system, a temperature-controlled quartz reactor containing our monolith catalyst, and an FTIR and micro-gas chromatograph (GC) for effluent gas analysis. Our catalytic reactor consisted of a 2.5 cm OD x 2.2 cm ID x 40 cm long quartz tube able to house a small monolithic piece (~2.1 cm dia. x 2.1 cm long, ~7 cm^3) of a degreened (16 hrs in air at 700°C in 10% H_2O at Oak Ridge National Laboratory) commercial lean NOx trap catalyst manufactured by Umicore (provided by Umicore through ORNL as part of the CLEERS activity). The Umicore catalyst in many ways resembles a three-way catalyst with added barium for storage. It contains the precious metals Pt, Pd and Rh (in descending quantities), added ceria and zirconia (for oxygen storage) and BaO for NOx storage. The barium loading is 20 wt% as BaO on Al_2O_3, and the targeted precious metal loading was 100 g/ft^3 of Pt/Pd/Rh in a 9:3:1 ratio.

Gas analysis was performed with FTIR (NO, NO_2, H_2O, NH_3, N_2O) and a micro GC (MTI analytical Quad series), with the latter used to detect H_2, O_2, and N_2, as well as N_2O (for calibration with results obtained by FTIR). For the GC data, approximately 65 seconds was required to elute all the gases present, which determined the shortest possible time between injections. Since the GC sampled the flow at only one instant during a cycle, it was necessary to control the lean-to-rich transition with respect to the GC injection over a series of identical cycles. By programming the total lean-rich cycle period to be slightly shorter than the GC repeat time, we were able to sample gas over the entire rich period and beyond.

A typical experiment was run as follows. By bypassing the catalyst, the inlet NOx concentration for both the rich and lean flow mixtures was determined. The gas was then passed over the catalyst and a series of lean-rich cycles were run. Using the FTIR to make nearly real-time measurements of the NO, NO_2, N_2O, H_2O and NH_3 concentrations, we waited until reproducible lean-rich cycles were obtained, which typically took between 10 and 60 minutes, then bypassed the FTIR and began the GC experiments. Unless otherwise noted, our experimental conditions were as follows. The total flow was two standard liters per minute over a 7 cm^3 coated catalyst brick for a calculated gas-hourly space velocity of ~17,000 hr^{-1}. The input NOx concentration was fixed at 280 ppm of NO during both cycles. Lean flow included 4% oxygen, while rich flow contained 1.3% hydrogen. The catalyst temperature was between 250 and 260ºC.

Results

Changing Morphology of BaO/Al_2O_3 during NO_2 Uptake and Release

Here we report on the cycle of morphology changes for BaO/Al_2O_3 NSR catalysts observed using TPD, FTIR and ^{15}N NMR spectroscopies, synchrotron TR-XRD, and TEM/EDS. As we will discuss below, the results of both TR-XRD and TEM analysis show that large $Ba(NO_3)_2$ crystallites are formed on the alumina support material during its preparation by an incipient wetness method using an aqueous $Ba(NO_3)_2$ solution. A large fraction of the alumina surface remains Ba-free after this procedure. Upon thermal treatment, these large $Ba(NO_3)_2$ crystallites decompose to form nanosized BaO particles. In fact, we propose that a thin BaO film (monolayer) forms on the alumina support, and the BaO nanoparticles are located on top of this interfacial BaO layer. During room-temperature NO_2 uptake, nanosized (<5 nm) $Ba(NO_3)_2$ particles form, and these particles are stable at room temperature. Heating the material to higher temperature (573 K) in the presence of NO_2 results in the formation of larger $Ba(NO_3)_2$ crystals (~15 nm). At higher temperatures, even in the absence of NO_2, the average particle size of $Ba(NO_3)_2$ crystallites increases further (~32 nm), and then, as $Ba(NO_3)_2$ decomposes, the nano-sized BaO particles reform.

For the purposes of this report, we only describe the changes occurring during catalyst preparation (details provided above) of a model 20 wt.% $Ba(NO_3)_2/Al_2O_3$ material, using TR-XRD and TEM/EDS to follow these changes. As detailed in [4], we performed similar experiments during the uptake and release of NO_2 onto the calcined catalyst material. From this full set of data, we propose the 'morphology cycle' described below.

A series of XRD patterns obtained during temperature-programmed decomposition of the as-prepared $Ba(NO_3)_2/Al_2O_3$ in a He flow is shown in Figure 1 in the 25-980°C temperature range. The room-temperature XRD pattern of the as-prepared and dried material contains peaks that can be assigned to crystalline $Ba(NO_3)_2$ and –alumina. Up to about 375°C, the characteristic diffraction peaks are practically unchanged, suggesting that the

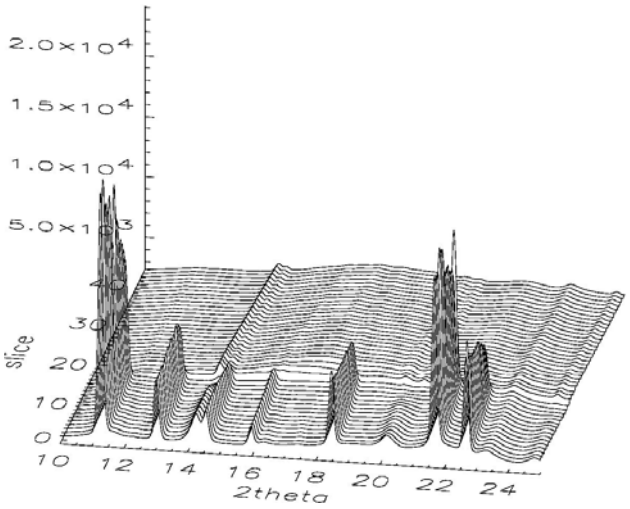

Figure 1. TR-XRD patterns collected during temperature-programmed decomposition from an as-prepared 20 wt.% $Ba(NO_3)_2/Al_2O_3$ sample.

$Ba(NO_3)_2$ crystallites are stable on the alumina surface in this temperature range. Heating the sample above 375°C results in a rapid decrease in the intensities of all $Ba(NO_3)_2$-related diffraction features. These results clearly indicate the complete decomposition of $Ba(NO_3)_2$ on the alumina surface by the time the sample temperature reaches 550°C, more than 100°C lower than the temperature reported for the decomposition of unsupported $Ba(NO_3)_2$ (>650°C). However, the results are in agreement with our previously reported data [6] in which we have shown that, due – most probably – to a strong oxide-oxide interaction, the $Ba(NO_3)_2$ phase that formed upon NO_2 uptake decomposed at much lower temperature than the unsupported bulk $Ba(NO_3)_2$. A more detailed analysis of the TR-XRD data (not shown here) yields the nitrate particle size as a function of sample temperature. Interestingly, the average particle size of about 60 nm does not change with sample temperature up to the point where the nitrate phase completely disappears. After the decomposition of the $Ba(NO_3)_2$ phase, only diffraction features of a nanocrystalline BaO phase and the alumina support can be seen. Increasing the sample temperature above 725°C results in the formation of a $BaAl_2O_4$ phase.

A TEM image from an as-prepared $Ba(NO_3)_2/Al_2O_3$ sample is shown in Figure 2 (left-hand side),

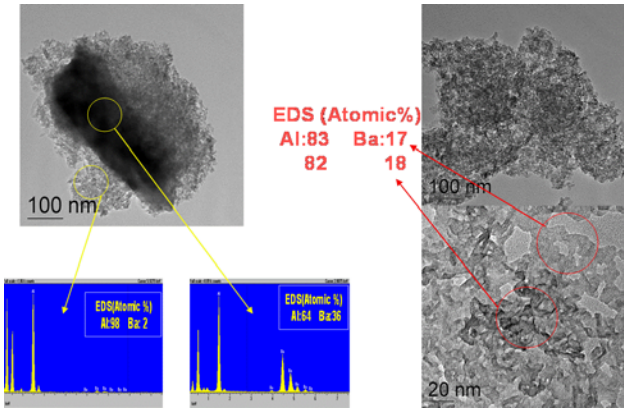

Figure 2. Left-hand side: Typical TEM image from the as-prepared $Ba(NO_3)_2/Al_2O_3$ sample (the precursor for the 20 wt% BaO/Al_2O_3 material). Below this image shows EDS spectra from two selected spots showing the very different compositions in these two regions of the sample. Right-hand side: TEM images from the 20 wt% BaO/Al_2O_3 sample after calcination in dry air at 500°C. The results of EDS analysis are again shown for two selected spots on the 20 wt% BaO/Al_2O_3 sample.

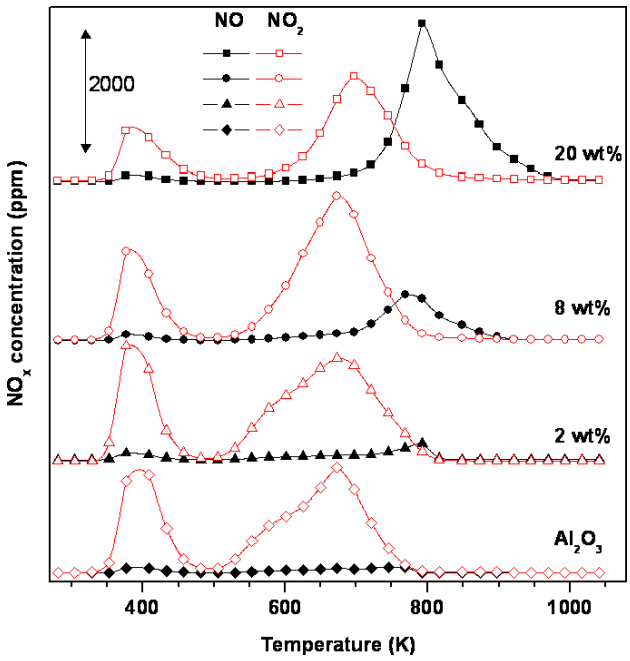

Figure 3. TPD spectra obtained after 30 minutes NO_2 adsorption at room temperature on different Ba-loaded catalysts calcined at 500°C.

where a large $Ba(NO_3)_2$ crystal can be seen on the alumina support. EDS results for two selected regions of this catalyst particle are also shown, with an analysis confirming that the large, dark-shaded crystal seen in the TEM image is $Ba(NO_3)_2$, while there is little, if any, Ba-containing phases elsewhere on the alumina support. From analyzing a number of other TEM images, we can say that large $Ba(NO_3)_2$ crystals (from tens of nanometers to hundreds of nanometers in size) form on the alumina support upon the incipient wetness catalyst preparation with an aqueous $Ba(NO_3)_2$ solution. Only a small fraction of the alumina surface is covered by these $Ba(NO_3)_2$ crystals, while most of the support is Ba-free. Upon heating the as-prepared and dried $Ba(NO_3)_2/Al_2O_3$ catalyst to 500°C in flowing dry air, the morphology of the resulting material closely resembles that of the alumina support (right side of Figure 2). EDS analysis of the 20 wt%-BaO/Al_2O_3 catalyst confirms the even distribution of Ba on the alumina support. The two spots analyzed (a light and a dark spot in the TEM image) show practically the same Al/Ba atomic ratios (83/17 and 82/18, respectively). As noted above, we performed similar *in-situ* TR-XRD and *ex-situ* TEM/EDS experiments during NO_2 uptake and release on the calcined 20 wt.% $Ba(NO_3)_2/Al_2O_3$ sample and used these data to propose the morphology model described below.

Temperature-programmed desorption (TPD) spectra acquired after NO_2 adsorption at 300 K for Al_2O_3 and 2 wt%, 8 wt%, and 20 wt% BaO/Al_2O_3 catalysts are shown in Figure 3 [6,7]. For the purposes of this summary, we only discuss the desorption peaks in the spectra that appear above 475 K because lower temperatures are not important for the practical operation of the NSR technology. There are two main high-temperature (>475 K) desorption peaks, corresponding to NO_2 and NO desorption at ~600 K and at ~800 K, respectively, that have been proposed to originate from the decomposition of monolayer (ML) and bulk barium nitrate phases, respectively [6]. Thus, it is especially notable in the spectra that the amount of NO desorption shows a strong correlation with Ba loading, as this result provides strong evidence for this previous assignment.

The FTIR spectra obtained from the 773K-calcined 2, 8 and 20 wt.% BaO/Al_2O_3 after NO_2 exposure at 300 K, displayed in Figure 4 and

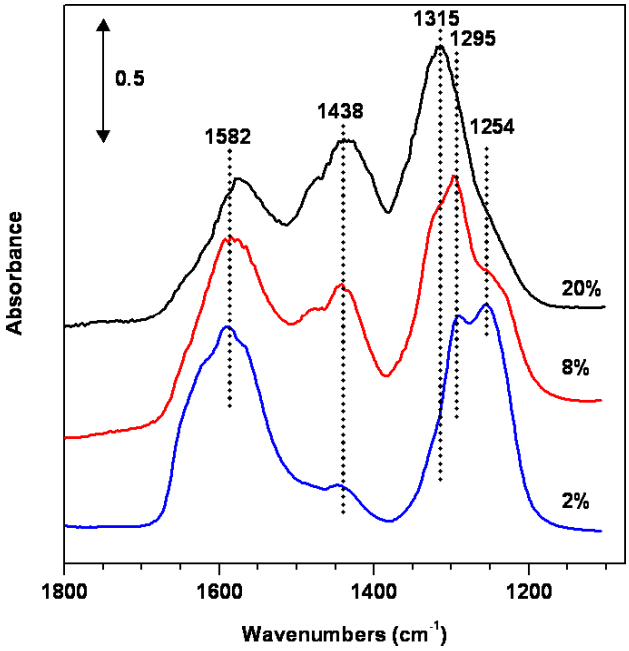

Figure 4. FTIR spectra after NO_2 adsorption at room temperature on different Ba-loaded catalysts calcined at 500°C.

in accord with those reported previously [6,8], can be understood in a similar way as the TPD results. On the Al_2O_3 support itself, two types of nitrates form upon NO_2 adsorption: so-called "bridging" (1234, 1250 cm^{-1} and 1595, 1620 cm^{-1}) and "chelating bidentate" (1300 cm^{-1} and 1570 cm^{-1}) nitrates (this nomenclature is based on comparing, or 'fingerprinting', the peak positions to spectra obtained from inorganic nitrates with known structures [8]). On BaO-containing samples, infrared features represent both "bidentate" (1300 and 1575 cm^{-1}) and "ionic" (1300 and 1420-1480 cm^{-1}) nitrates. We have further clarified the nature of these nitrate species by identifying the "ionic nitrates" as arising from a bulk $Ba(NO_3)_2$ phase while the "bidentate nitrates" were assigned to surface Ba-nitrate species [6]. In the data shown in Figure 4, note especially that the relative intensity of the infrared features representing the bulk ("ionic") nitrate peaks between 1300 and 1500 cm^{-1} increase with BaO coverage. Thus, these FTIR results are fully consistent with the TPD results shown in Figure 3 indicating the presence of two distinct morphologies for barium nitrate on alumina, a 'monolayer' phase that wets the alumina surface and bulk 3-d crystallites of $Ba(NO_3)_2$.

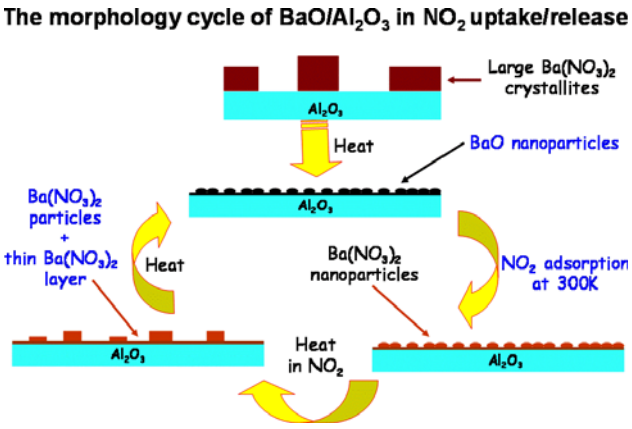

Figure 5. Schematic of the cycle of morphology changes taking place during NO_2 uptake and release on BaO/Al_2O_3 NOx storage/reduction materials.

From the just-described results, we have proposed [4] a model, schematically illustrated in Figure 5, for the morphology changes occurring in an LNT during synthesis and during operation under lean-NOx cycling conditions. The as-prepared $Ba(NO_3)_2/Al_2O_3$ material consists of large (>60 nm) $Ba(NO_3)_2$ crystallites positioned on the Al_2O_3 support. Most of the support surface is Ba-free. Heating this material to temperatures above 500°C results in the complete decomposition of the $Ba(NO_3)_2$ phase and the formation of a thin film layer of BaO, with BaO nanoparticles on top of this layer. The thus formed BaO/Al_2O_3 catalyst adsorbs NO_2 at 25°C without changing the morphology of the system; *i.e.*, small, nano-sized $Ba(NO_3)_2$ crystallites form. Conducting the NO_2 uptake at a higher temperature (200-500°C) results in the agglomeration of the small $Ba(NO_3)_2$ crystallites with an average particle size of ~15 nm. In the resulting $Ba(NO_3)_2/Al_2O_3$ system, we can detect Ba all over the alumina support, while in the as-prepared one there was only a fraction of the alumina support surface that was actually covered with $Ba(NO_3)_2$ crystals. Thus, the thin BaO ('monolayer') film adsorbs NO_2 as well, forming a stable $Ba(NO_3)_2$ 'monolayer' in addition to $Ba(NO_3)_2$ particles, as depicted at the bottom of Figure 5. We believe that this thin $Ba(NO_3)_2$ layer ('monolayer') is responsible for the low-temperature NO_2 desorption feature we have observed in the TPD results described above. After the decomposition of this thin $Ba(NO_3)_2$ layer to reform a thin BaO layer, the

remaining $Ba(NO_3)_2$ particulate phase decomposes in the same way as unsupported, bulk $Ba(NO_3)_2$, *i.e.*, by releasing $2NO+3/2O_2$ and reforming (~5 nm) BaO nanoparticles.

Nitrogen Balance Experiments

In an LNT catalyst system, the release and reduction of NOx occurs over a very short period. The speed of the NOx release and reduction creates difficulties in analyzing the chemistry using normal analytical techniques, which are typically better suited to slower, steady-state studies. We have investigated [5] the time dependence of NO, NO_2, NH_3, N_2O and N_2 released by an LNT catalyst using a combination of FTIR and gas chromatographic techniques. Di-nitrogen (N_2) was detected with the GC by using He rather than N_2 as the background gas. The FTIR was used not only to monitor NO, NO_2, NH_3 and N_2O, but also to establish cycle-to-cycle reproducibility. Under these conditions, we used the GC to sample the effluent at multiple times over many lean-rich cycles. To the extent that the chemistry was truly periodic and reproducible, we obtained the time dependence of the release of nitrogen after the lean-to-rich transition. Similar information was obtained for O_2, H_2 and N_2O. Combining the FTIR and GC data, we obtained good cycle-averaged nitrogen balances, indicating that all the major products were accounted for.

An example set of FTIR(a) and GC(b) data, for the case of a 67-20 second lean-rich cycle, is shown in Figure 6. In this particular case, NO and NO_2 are not plotted because no NOx was detected at any point during the lean-rich cycle. Upon switching to rich conditions, on the FTIR (Figure 6a) we observed an immediate pulse of N_2O followed by a distinctly slower appearance of H_2O, and after 10 seconds or so, the appearance of the undesirable product, NH_3, as well. On the GC (Figure 6b), we saw a rapid rise and fall of N_2 upon switching to rich conditions, with a full width-half maximum (FWHM) of ~5 seconds. The nitrogen signal leveled off to a small but non-zero value, consistent with an on-set of 'steady-state' "3-way"-like catalysis – namely, the reduction of incoming NOx by H_2 on the precious-metal components of the catalyst. Figure 6b also shows that, approximately 10 seconds into the rich cycle, oxygen essentially disappeared and hydrogen appeared. Comparing the GC and FTIR traces, we

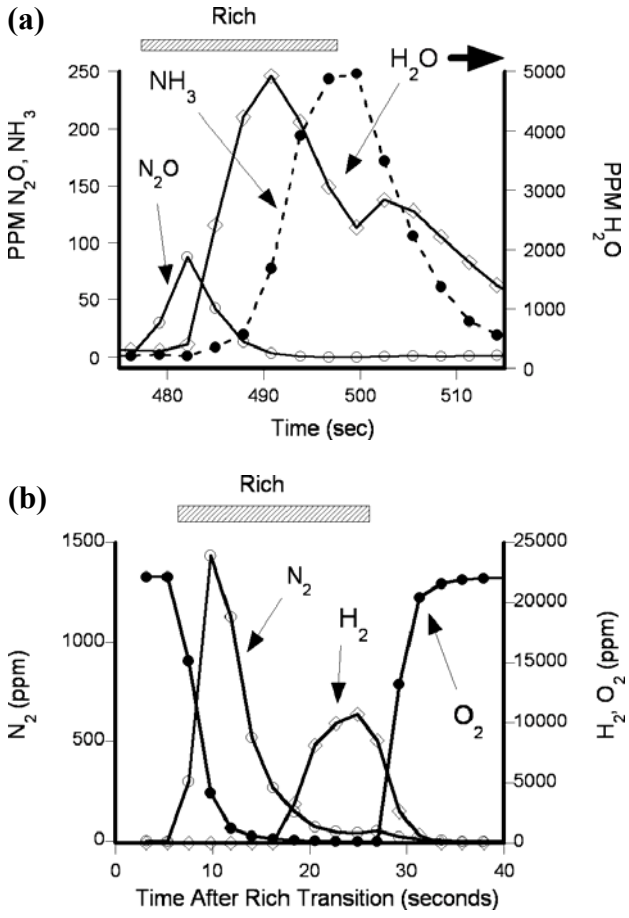

Figure 6. Products detected by FTIR (a) and GC (b) for a lean/rich cycle of 67/20 seconds. The box labeled Rich at the top of each plot represents the width of the rich period. Rich flow: 1.3% H_2, 270 ppm NO, balance He. Lean flow: 4% O_2, 270 ppm NO, balance He.

note that the H_2 and NH_3 signals were very similar. Both products appeared after gas-phase oxygen was gone and rose toward their 'steady-state' values until the switch back to lean conditions occurred. We also note that a large amount of H_2O was produced as long as excess oxygen was present. The H_2O concentration peaked approximately 10 seconds into the rich cycle and then dropped smoothly until the beginning of the subsequent lean period. At that point, a small upward spike in the H_2O signal was observed, presumably due to the reaction of O_2 with H_2 left over on the catalyst from the rich flow. Evidently, N_2O and N_2 are formed immediately after the lean-to-rich transition and are the primary N-containing products from stored NOx.

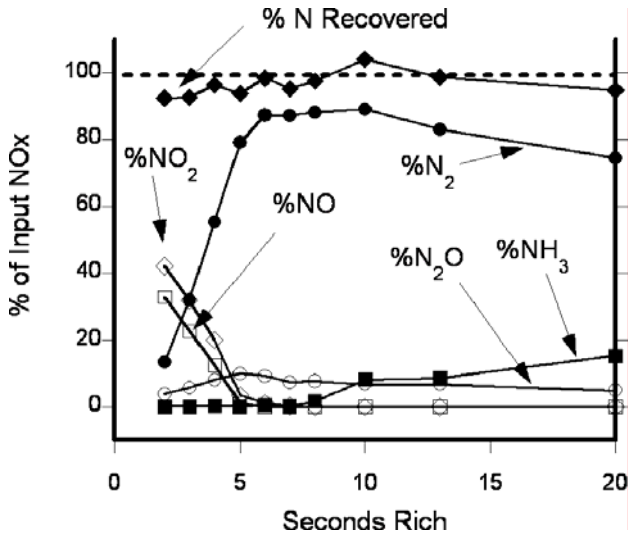

Figure 7. The complete set of analytical results for the N-containing products from a series of lean/rich cycle times, with the lean period fixed at 67 seconds and the rich time varied from 2-20 seconds.

We ran a series of experiments in precisely the same manner, but with varying rich periods. We collected data for a 67-second lean period followed by rich periods ranging from 2 to 20 seconds, with Figure 7 summarizing the entire data set in terms of % NOx conversion. As the rich period increased from 2 to 6 seconds, the amount of NOx surviving the catalyst dropped rapidly to zero, where it remained for all longer rich period cycles. Over the same changing rich-period range, the amount of N_2 produced increased rapidly and then leveled off, with essentially no further increase at rich times longer than ~5-6 seconds. The amount of N_2O went up from 2 to 5 seconds rich and then was level or perhaps tailed off slightly over the rest of the range. Ammonia appeared at measurable levels only in cycles with 8-second or longer rich periods and monotonically increased with the length of the rich period. The formation of N_2 was obviously reductant-limited up to rich cycles of 5 seconds or so. However, lengthening the rich period beyond 5 or 6 seconds didn't significantly increase the amount of N_2 produced, indicating that at the optimum point, the gas-phase concentration of reductant and the amount of stored NOx were well balanced. This result is valid only for the precise conditions we used; varying the hydrogen concentration could conceivably change the rich time required for optimum NOx reduction, although we haven't addressed that issue to date. The addition of H_2O and CO_2 will doubtless change the optimum conditions as well. It is especially notable that the reduction of stored NOx yields primarily N_2, with only small amounts of N_2O formed. Importantly, NH_3 was not observed at all during an optimized lean-rich cycle, but only appeared during very long rich periods. This implies that the H-atom surface concentrations on the precious metal are relatively small until the stored NOx is reduced. The appearance of NH_3 indicates no further gains can be obtained by further lengthening the rich period.

Conclusions

In this annual report, we have summarized two significant results that have been obtained in the first year of this project.

We described the cycle of morphology changes for BaO/Al_2O_3 NSR catalysts using synchrotron TPD, FTIR, TR-XRD, TEM and EDS. The results showed that large $Ba(NO_3)_2$ crystallites are formed on the alumina support material during its preparation by an incipient wetness method using an aqueous $Ba(NO_3)_2$ solution. A large fraction of the alumina surface remains Ba-free after this procedure. Upon thermal treatment, these large $Ba(NO_3)_2$ crystallites decompose to form nano-sized BaO particles. In fact, we propose that a thin BaO film (monolayer) forms on the alumina support, and the BaO nanoparticles are located on top of this interfacial BaO layer. During room-temperature NO_2 uptake, nanosized (<5 nm) $Ba(NO_3)_2$ particles form, and these particles are stable at room temperature. Heating the material to higher temperature (300°C) in the presence of NO_2 results in the formation of larger $Ba(NO_3)_2$ crystals (~15-30 nm). At still higher temperatures, as $Ba(NO_3)_2$ decomposes, the nano-sized BaO particles reform.

The reduction of stored NOx by H_2 in a commercial LNT catalyst has been shown, for the first time, to produce mainly N_2 with smaller quantities of N_2O. For insufficiently long rich periods, the adsorbed NOx builds up until the lean-cycle NOx storage is drastically reduced, degrading the overall performance significantly. Under these

conditions, the catalyst never fully removes stored NOx, and NO and NO_2 are observed throughout the entire lean-rich cycle. During overly long rich periods, NOx is never observed, but unfortunately, NH_3 is. Compared to an optimized rich cycle length, similar amounts of N_2 are produced early in the rich period, but its production drops off significantly once the stored NOx is depleted. Thus, the appearance of ammonia is an excellent indication that nitrogen production from stored NOx is complete, and that the optimal rich period has been reached or exceeded. Importantly, the proper choice of the rich period length prevented the production of significant amounts of NH_3 altogether. Under our conditions, a small but noticeable amount of N_2O was unavoidably produced.

FY 2005 Presentations

Invited

1. C.H.F. Peden (invited presenter), "Fundamental Studies of Catalytic NOx Vehicle Emission Control", Presentation at the University of Pennsylvania, Philadelphia, PA, October, 2004.
2. C.H.F. Peden (invited presenter), "The Adsorption and Reaction of NOx (NO and NO_2) on BaO/Al_2O_3 Storage/Reduction Materials", presentation at the 2005 Meeting of the Pacific Coast Catalysis Society, Berkeley, CA, March, 2005.
3. J. Szanyi (invited presenter), J.H. Kwak, D.H. Kim, J.C. Hanson, and C.H.F. Peden, "Nature of Nitrate Species on BaO/Al_2O_3 NSR Catalysts", presentation at the ACS National Meeting, San Diego, CA, March, 2005.

Contributed

4. J.H. Kwak, D.H. Kim, J. Szanyi, T. Szailer, and C.H.F. Peden, "Reactivity of $Pt/BaO/Al_2O_3$ for NOx Storage/Reduction: Effects of Pt and Ba Loading", presentation at the 229th National Meeting of the American Chemical Society, San Diego, CA, March, 2005.
5. R.S. Disselkamp, D.H. Kim, J.H. Kwak, C.H.F. Peden, J. Szanyi, and R.G. Tonkyn, "Fundamental Studies of NOx Adsorber Materials", presentation at the National Laboratory Advanced Combustion Engine R&D Merit Review and Peer Evaluation, Argonne, IL, April, 2005.
6. J. Szanyi, J.H. Kwak, S.D. Burton, J.A. Rodriguez, and C.H.F. Peden, "Spectroscopic Characterization of NOx Species on Na-, and Ba-Y, FAU Zeolites", presentation at the 19th National American Meeting of the Catalysis Society, Philadelphia, PA, May, 2005.
7. J.H. Kwak, D.H. Kim, J. Szanyi, T. Szailer, and C.H.F. Peden, "Reaction Studies on $Pt/BaO/Al_2O_3$ for NOx Storage/Reduction Catalysts", presentation at the 19th National American Meeting of the Catalysis Society, Philadelphia, PA, May, 2005.
8. R.G. Tonkyn, R.S. Disselkamp, and C.H.F. Peden, "Mechanistic Studies of the Reduction of Stored NOx on BaO/Al_2O_3-Based Lean-NOx Traps", presentation at the 19th National American Meeting of the Catalysis Society, Philadelphia, PA, May, 2005.
9. R.S. Disselkamp, R.G. Tonkyn, Y.-H. Chin, and C.H.F. Peden, "A Multiple-Site Kinetic Model to Simulate $O_2 + 2\ NO \rightleftharpoons 2\ NO_2$ Oxidation-Reduction Chemistry on Pt(100) Catalysts", presentation at the 60th NORM, Pacific N.W. Regional American Chemical Society (ACS) meeting, Fairbanks, AK, June, 2005.
10. D.H. Kim, J.H. Kwak, C.H.F. Peden, T. Szailer, J.C. Hanson, and J. Szanyi, "Morphology and Composition Cycle of BaO/Al_2O_3 NSR Catalysts during NO_2 Uptake and Release: A Multi Spectroscopy and Microscopy Study", presentation at the 2005 Diesel Engine Emissions Reduction Conference, Chicago, IL, August, 2005.

FY 2005 Publications

1. Szanyi, J.; Kwak, J.H.; Hanson, J.; Wang, C.M.; Szailer, T.; Peden, C.H.F. "The Changing Morphology of BaO/Al_2O_3 during NO_2 Uptake and Release." J. Phys. Chem. B **109** (2005) 7339-7344.
2. Szanyi, J.; Kwak, J.H.; Kim, D.H.; Burton, S.; Peden, C.H.F. "NO_2 Adsorption on BaO/Al_2O_3: the Nature of the Nitrate Species." J. Phys. Chem. B **109** (2005) 27-29.
3. Szanyi, J.; Kwak, J.-H.; Kim, D.-H.; Hanson, J.C.; Peden, C.H.F. "Nature of Nitrate Species on BaO/Al_2O_3 NSR Catalysts." Preprints of the Fuel Division of the American Chemical Society **50(1)** (2005) 392-393.
4. Kwak, J.-H.; Kim, D.-H.; Szanyi, J.; Szailer, T.; Peden, C.H.F. "Reactivity of $Pt/BaO/Al_2O_3$ for NOx Storage/Reduction: Effects of Pt and Ba Loading." Preprints of the Fuel Division of the American Chemical Society **50(1)** (2005) 400-401.
5. Szailer, T.; Kwak, J.H.; Kim, D.H.; Szanyi, J.; Wang, C.; Peden, C.H.F. "Effects of Ba Loading and Calcination Temperature on $BaAl_2O_4$ Formation for Ba/Al_2O_3 Storage and Reduction Catalysts." Catal. Today, in press.

6. Tonkyn, R.G.; Disselkamp, R.S.; Peden, C.H.F. "Nitrogen Release from a NOx Storage and Reduction Catalyst." Catal. Today, in press.
7. Szailer, T.; Kwak, J.H.; Kim, D.H.; Hanson, J.; Peden, C.H.F.; Szanyi, J. "Reduction of Stored NOx on Pt/Al_2O_3 and $Pt/BaO/Al_2O_3$ Catalysts with H_2 and CO." J. Catal., submitted for publication.
8. Disselkamp, R.S.; Tonkyn, R.G.; Chin, Y.-H.; Peden, C.H.F. "A Multiple-Site Kinetic Model to Simulate O_2 + 2 NO 2 NO_2 Oxidation-Reduction Chemistry on Pt(100) Catalysts." J. Catal., submitted for publication.

References

1. (a) Miyoshi, N., Matsumoto, S., Katoh, K., Tanaka, T., Harada, J., Takahashi, N., Yokota, K., Sugiura, M., Kasahara, K. SAE Paper 950809, 1995; (b) Miyoshi, N., Matsumoto, S. Sci. Technol. Catal., 1998, 245.
2. Epling, W.S.; Campbell, L.E.; Yezerets, A.; Currier, N.W.; Parks, J.E. Catal. Rev.–Sci. Eng., 2004, 46, 163.
3. Wang, X., Hanson, J.C., Frenkel, A.I., Kim, J.-Y., Rodriguez, J.A. J. Phys. Chem. B, 2004, 108, 13667.
4. Szanyi, J., Kwak, J.H., Hanson, J.C., Wang, C.M., Szailer, T., Peden, C.H.F. J. Phys. Chem. B, 2005, 109, 7339.
5. Tonkyn, R.G., Disselkamp, R.S., Peden, C.H.F. Catal. Today, in press.
6. Szanyi, J., Kwak, J.H., Kim, D.H., Burton, S., Peden, C.H.F. J. Phys. Chem. B, 2005, 109, 27.
7. Szailer, T., Kwak, J.H., Kim, D.H., Szanyi, J., Wang, C., Peden, C.H.F. Catal. Today, in press.
8. Prinetto, F., Ghiotti, G., Nova, I., Lietti, L., Tronconi, E., Forzatti, P. J. Phys. Chem. B, 2001, 105, 12732.

II.B.2 Mechanisms of Sulfur Poisoning of NOx Adsorber Materials

Do Heui Kim, Ya-Huei Chin, George Muntean, Chuck Peden (Primary Contact)
Pacific Northwest National Laboratory (PNNL)
P.O. Box 999, MS K8-93
Richland, WA 99352

DOE Technology Development Manager: Ken Howden

CRADA Partners:
Randy Stafford, John Stang, Alex Yezeretz, Bill Epling, Neal Currier - Cummins Inc.
Hai-Ying Chen, Howard Hess, Dave Lafyatis - Johnson Matthey

Objectives

- Develop and apply characterization tools to probe the chemical and physical properties of NOx adsorber catalyst materials for studies of deactivation due to sulfur poisoning and/or thermal aging. Utilize this information to develop mechanistic models that account for NOx adsorber performance degradation.
- Develop protocols and tools for failure analysis of field-aged materials.
- Provide input on new catalyst formulations; verify improved performance through materials characterizations and laboratory and engine testing.

Approach

- In collaboration with Johnson Matthey researchers, synthesize and process (via various thermal aging and SO_2 treatment protocols) 'Simple Model' and 'Enhanced Model' NOx adsorber materials.
- Utilize PNNL's state-of-the-art surface science and catalyst characterization capabilities, such as x-ray diffraction (XRD), transmission electron microscopy (TEM)/energy dispersive spectroscopy (EDS), x-ray photoelectron spectroscopy (XPS), temperature-programmed desorption (TPD)/thermal gravimetric analysis (TGA), and Brunauer-Emmett-Teller (BET)/pore size distribution, as well as performance testing facilities to examine the NOx storage chemistry and deactivation mechanisms on the 'Simple' and 'Enhanced' model materials.

Accomplishments

- Detailed in-situ XRD studies coupled with performance measurements have shown that thermal deactivation can be most directly correlated with Pt particle size growth, which can also be used to explain dramatic differences in the behavior of 'Simple Model' and 'Enhanced Model' lean NOx trap (LNT) materials.
- Studies of H_2O treatment applied to 'fresh' and thermally deactivated 'Simple Model' LNT materials demonstrated the segregation of barium carbonates from the alumina support irrespective of the initial phase (*i.e.*, highly dispersed barium carbonate or barium aluminate). These results have implications for LNT material synthesis and for LNT operation.
- As noted by others, we find that thermal deactivation is very sensitive to the atmosphere (*i.e.*, oxidizing or reducing). Some indications for why this is so have been determined.
- Demonstrated that TPD of NO_2 can be used to assess the morphology of Ba 'sites' that are being deactivated thermally or by sulfur poisoning. Similarly, the nature of the sulfur species adsorbed with exposure time can be qualitatively assessed by temperature-programmed reduction (TPR) with H_2.

- Comparisons of the performance of 'Simple Model' and 'Enhanced Model' LNT materials as a function of sulfur exposure have been made.
- Deconvoluted two deactivation sources (thermal aging and sulfur aging) by applying a new reaction protocol. This allows unambiguous identification of conditions when one or both of these mechanisms are responsible for deactivation. Furthermore, clear differences in the behavior of the 'Simple Model' and 'Enhanced Model' LNT materials can now be specifically attributed to relative sensitivities to sulfur and/or thermal deactivation processes.
- Detailed studies of the process of 'regeneration' following sulfur poisoning have been initiated.
- Three public presentations and one manuscript have been cleared for release by Cooperative Research and Development Agreement (CRADA) partners. The manuscript, submitted to the journal, Catalysis Today, has now been accepted for publication.

Future Directions

- Further refine function-specific measures of 'aging':
  - More detailed studies to verify that techniques such as NO_2 TPD and H_2 TPR are providing information content suggested by studies to date.
  - Some effort still to identify new approach to unravel some key unknowns (*e.g.*, role of precious metal/storage material 'contact').
- Validate most suitable function-specific measures on samples incrementally 'aged' under realistic conditions.
- Confirm 'protocol' on engine 'aged' samples.

Introduction

The NOx adsorber (also known as lean NOx trap – LNT) technology is based upon the concept of storing NOx as nitrates over storage components, typically barium species, during a lean-burn operation cycle and then reducing the stored nitrates to N_2 during fuel-rich conditions over a precious metal catalyst [1]. This technology has been recognized as perhaps the most promising approach to meet stringent NOx emissions standards for diesel vehicles within the Environmental Protection Agency's (EPA's) 2007/2010 mandated heavy-duty engine emission regulations. However, problems arising from either thermal or SO_2 deactivation, or both, must be addressed to meet durability requirements. Therefore, an understanding of these processes will be crucial for the development of the LNT technology.

This project is focused on the identification and the understanding of the important degradation mechanism(s) of the catalyst materials used in LNTs. 'Simple Model' and 'Enhanced Model' Pt/BaO/Al_2O_3 samples are being investigated. In particular, the changes in physicochemical properties related to the reaction performances of these LNT materials, due to the effects of high-temperature operation and sulfur poisoning, are the current focus of the work. By comparing results obtained on 'Simple Model' Pt/BaO/Al_2O_3 with 'Enhanced Model' materials, we try to understand the role of various additives on the deactivation processes. However, this report covers primarily the results obtained in FY 2005 on the 'Simple Model' Pt/BaO/Al_2O_3 materials for proprietary reasons. We further note here that while project progress for the entire year is summarized above in the "Accomplishments" section, we present below more detail about results in two specific areas: i) the correlation of Pt particle size growth with deactivation; and ii) highlights of the studies on sulfur poisoning obtained this last year.

Approach

In a newly constructed microcatalytic reactor system (Figure 1a), LNT performance is evaluated in a fixed bed reactor operated under continuous lean-rich cycling. Rapid lean-rich switching is enabled just prior to the elevated temperature zone (furnace)

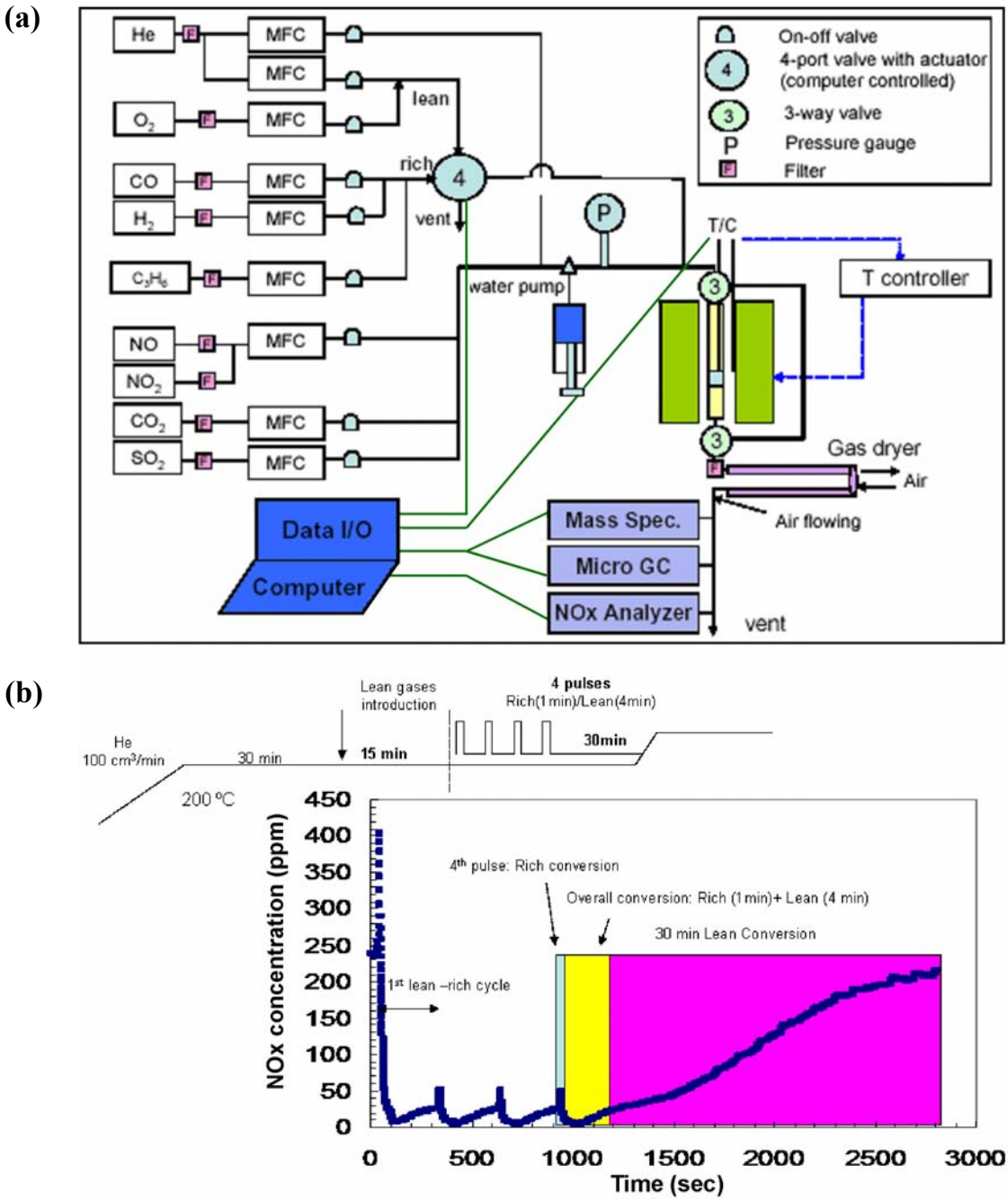

Figure 1. (a) A schematic of the microreactor constructed for this project's studies, and (b) a common reaction protocol used here along with example data where the performance assessments are defined.

where the LNT materials are contained in quartz tubing. After removing water, the effluent of the reactor can be analyzed by mass spectrometry, gas chromatography, and by a chemiluminescent NOx analyzer. A typical baseline performance testing protocol is illustrated in Figure 1b. In this case, the sample is heated to a reaction temperature in flowing He, the feed switched to a 'lean-NOx' mixture containing oxygen and NO, as well as CO_2 and/or H_2O. After an extended period (15 minutes or more), multiple rich/lean cycles of 1- and 4-minute duration, respectively, are run and NOx removal performance is assessed after at least 3 of these are completed. In the LNT technology, the state of the

system is constantly changing so that performance depends on when it is measured. As such, we measure NOx removal efficiencies in at least three different ways, as illustrated in Figure 1b. "Lean conversion (4 minutes)" and "lean conversion (30 minutes)" measure NOx removal efficiencies for the first 4 minutes and first 30 minutes of the lean period, respectively.

In addition, material treatments such as SO_2 aging and post-mortem catalyst characterizations are conducted in the same test stand without exposing the catalyst sample to air. We have established a reaction protocol which evaluates the performance of samples after various thermal aging and sulfation conditions. In this way, we are able to identify optimum desulfation treatments to rejuvenate catalyst activities.

State-of-the-art catalyst characterization techniques such as XRD, XPS, TEM/EDS, BET/pore size distribution, and temperature-programmed desorption/reaction (TPD/TPRX) are utilized to probe the changes in physicochemical properties of the catalyst samples under deactivating conditions; *e.g.*, thermal aging and SO_2 treatment. Specifically, H_2 TPRX (temperature-programmed reaction), NO_2 TPD and XPS methods are used extensively to quantify the levels, speciation and distribution of sulfur on the adsorber material as a function of exposure time.

Results

Correlation of Pt particle size with the NOx storage performance during thermal aging

We established a direct relationship between Pt particle size and NOx storage performance by correlating the results of *in-situ* time-resolved XRD, TEM, and Fourier transform infrared (FTIR) measurements after CO adsorption with NOx storage performance measurements for samples treated under oxidizing conditions at elevated temperature (700, 800 and 900°C). *In-situ* XRD results provided direct evidence and established the temperature range at which growth of Pt particles occurs. As demonstrated in Figure 2, we obtained the change of Pt crystallite size and the total peak area for the major Pt XRD peak of the 'Simple Model' LNT

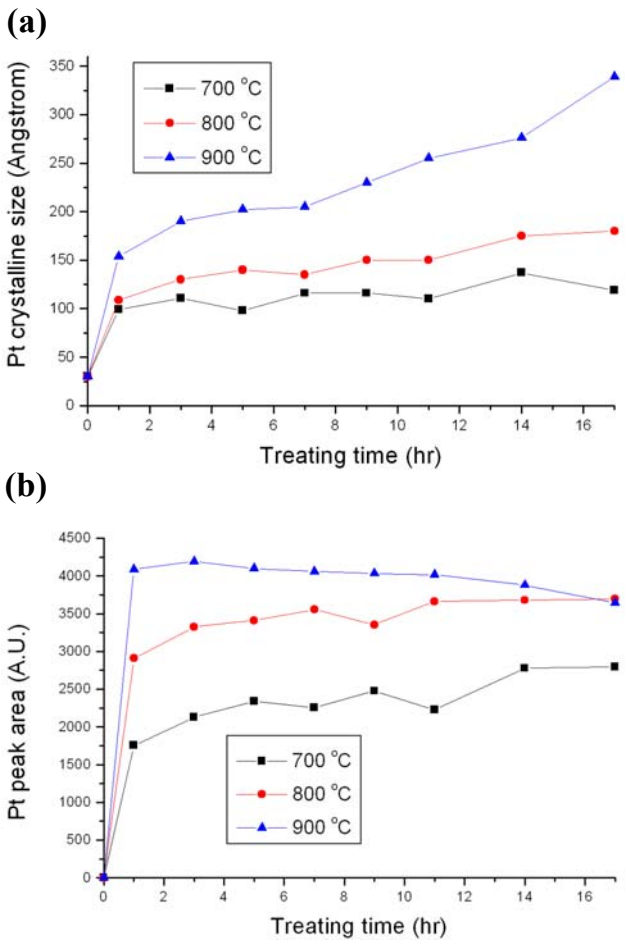

Figure 2. (a) Change of the Pt particle crystallite size, obtained using the Scherrer equation on the *in-situ* XRD data for the 'Simple Model' catalyst, as a function of calcination temperature and treatment time. (b) A plot of the total area of a principle XRD Pt peak as a function of calcination temperature and time.

sample by analyzing the Pt(111) peak using the Scherrer equation. For all calcination temperatures studied, Pt crystallite size increases abruptly within 1 hr, followed by the steady growth with time. As the temperature increases, the rate of Pt phase growth increases. Both CO adsorption and TEM results were entirely consistent with the *in-situ* XRD data. These results are also in good agreement with previous studies [2] that concluded that Pt sintering rates are exponentially dependent on temperature and linearly on time. Figure 3 shows the activity results of the same sample obtained following similar thermal treatments for various times at 700, 800 and

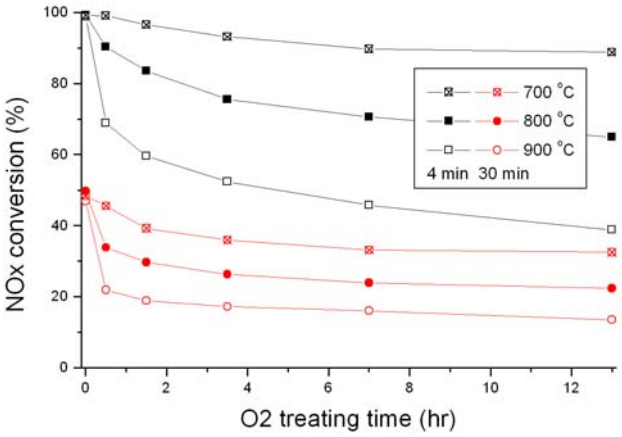

Figure 3. Change of NOx storage performance (4 min and 30 min conversion) as a function of calcination temperature and time.

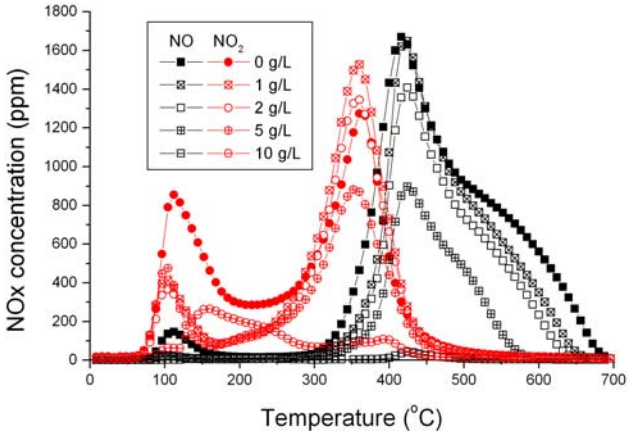

Figure 4. *In situ* NO_2 TPD from the 'Simple Model' LNT sample as a function of degree of sulfation.

900°C. With increasing calcination temperatures, the NOx conversion decreases significantly. Note especially that NOx conversion drops significantly within 1 hour, followed by a slower decrease with oxygen treatment time. Recalling the just-described results from the *in-situ* XRD experiments, we find that the NOx storage performance can be directly correlated with the changing Pt particle size; more specifically, greater NOx storage performance is observed for samples with small-sized Pt particles, and performance deteriorates rapidly as the Pt particles sinter during the thermal treatment. For the case of the 'Enhanced Model' sample in which Pt sintering is inhibited to a large extent, the NOx storage performance is maintained to higher temperatures relative to the 'Simple Model', providing further support for the conclusion that the inhibition of Pt sintering at elevated temperature is a key factor to designing more durable NOx adsorber catalysts.

Effect of sulfation on the NOx storage/release performance

NOx storage performance for both 'Simple Model' and 'Enhanced Model' materials is initially affected minimally and then decreases gradually as sulfation proceeds (*i.e.*, when SO_2 is present in the reaction mixture), in good agreement with previous results [3]. In order to directly investigate the interaction of NOx with the two LNT materials as a function of sulfation, we performed *in situ* NO_2 TPD after varying degrees of sulfation, as shown in Figure 4. According to results from other studies we have carried out [4], NO_2 and NO desorption can be assigned to the decomposition of 'monolayer' and 'bulk-like' forms of barium nitrates, respectively. By integrating the NO_2 and NO peaks for the data shown in Figure 4, we find that the decomposition of 'bulk' barium nitrates monotonically decreases with sulfation, while 'monolayer' barium nitrates are essentially unaffected at low sulfur levels. From this, it seems that 'monolayer' Ba species may be more important in determining LNT performance than the 'bulk' ones. We also carried out *in-situ* H_2 TPRX after the different degrees of sulfation. The sulfur species deposited during the early stage of sulfation are stable even up to 900°C. We also note that the 'Enhanced Model' sample displays distinctly superior desulfation behavior at lower temperature, such that it recovers activity more completely than the 'Simple Model' catalyst after identical desulfation treatments.

Reaction protocol to de-couple effects of thermal aging and desulfation

In order to regenerate the LNT catalysts to remove sulfate species that poison the material, a high-temperature desulfation process is required. Physical and chemical property changes in the material due to removal of sulfates and/or due to the required high temperatures of desulfation are unavoidable. Thus, there is a trade-off in

regenerating activity by removing the sulfur species while, on the other hand, potentially decreasing it due to thermal deactivation. Furthermore, it becomes difficult to distinguish what is responsible for deactivation in this case. Therefore, a reaction protocol was established to de-couple these two effects. After running the reaction in the presence or absence of SO_2, the catalyst was treated at higher temperature, followed by a 2nd evaluation of the activity without SO_2. Comparison of the activities with/without SO_2 and before/after the higher-temperature 'desulfation' treatment allowed us to estimate the contribution to the activity changes from the two potential sources of deactivation. The NOx conversions of both the 'Simple Model' and 'Enhanced Model' LNTs start to decline above 700°C in the absence of SO_2 in the reactant gas mixture due to thermal deactivation (Pt sintering as shown above). When SO_2 is added to the reactant, it appears that the conversion after desulfation follows that of thermally aged samples above 700°C, indicating that the desulfation is essentially complete above this temperature and that deactivation is due to thermal aging. On the other hand, the 'Enhanced Model' LNT shows more complete recovery of performance at lower temperatures than the 'Simple Model' material, where the thermal aging does not occur to a significant extent. In addition, XPS analysis of post-reaction samples showed that the 'Enhanced Model' sample shows a more rapid decrease of sulfur species as sulfate on the surface than the 'Simple' one, which can explain their differing performance observed after the desulfation process. Thus, we have shown that our new reaction procotol allows for the decoupling of thermal aging and sulfur effects, allowing for the identification of optimum conditions where the thermal aging is minimized while the desulfation is correspondingly maximized.

Conclusions

PNNL and its CRADA partners from Cummins Inc. and Johnson Matthey are carrying out a project to study the mechanisms of deactivation of the materials proposed for use in lean NOx traps (LNTs) arising from thermal aging and SO_2 poisoning. Results demonstrate that when thermal aging is applied to the LNT catalyst, Pt crystallite size plays a critical role in determining the NOx storage activity, which implies that the development of a catalyst that is highly durable against Pt sintering is desirable. Also of practical importance is to minimize high-temperature excursions since the growth rate of Pt particles is dependent exponentially on the temperature. It was found that the SO_2 affected NOx adsorption/desorption chemistry differently depending on the materials. By using a novel reaction protocol to de-couple thermal deactivation and desulfation, it was found that the 'Enhanced Model' LNT material possesses the ability to de-sulfate at lower temperature where Pt sintering is minimized, thus recovering NOx storage performance more readily and completely after deactivation due to sulfur poisoning. In conclusion, our results provide some important design and/or operation criteria for NOx adsorber systems in order to achieve lower deactivation that arises from sulfation and thermal sintering.

FY 2005 Publications/Presentations

1. D.H. Kim, Y.-H. Chin, J.H. Kwak, J. Szanyi, and C.H.F. Peden, "Segregation of Ba Phase in BaO/Al_2O_3 upon H_2O Treatment", presentation at the American Institute of Chemical Engineers (AIChE) Annual Meeting, Austin, TX, November, 2004.
2. D.H. Kim, Y.-H. Chin, G.G. Muntean, C.H.F. Peden, N. Currier, B. Epling, R. Stafford, J. Stang, A. Yezerets, H.-Y. Chen, and H. Hess, "Mechanisms of Sulfur Poisoning of NOx Adsorber Materials", presentation at the DOE Combustion and Emission Control Review, Argonne, IL, April, 2005.
3. D.H. Kim, Y.-H. Chin, G.G. Muntean, C.H.F. Peden, R.J. Stafford, J. Stang, A. Yezerets, W.S. Epling, N. Currier, H. Chen, H. Hess, O. Kresnawahjuesa, and D. Lafyatis, "Investigations of SO_2 Poisoning and Thermal Aging Mechanisms for Pt/BaO/Al_2O_3 Lean NOx Trap Catalysts", presentation at the 19th North America Meeting on Catalysis, Philadelphia, PA, May, 2005.
4. A. Yezerets, N. Currier, W.S. Epling, D.H. Kim, C.H.F. Peden, G.G. Muntean, C.M. Wang, S.D. Burton, and R.L. Vander Wal, "Toward Fuel Efficient DPF Systems- Understanding the Soot Oxidation Process", presentation at the 2005 Diesel Engine Emissions Reduction Conference, Chicago, IL, August, 2005.
5. D.H. Kim, Y.-H. Chin, G.G. Muntean, C.H.F. Peden, K. Howden, R.J. Stafford, J.H. Stang, A. Yezerets, W.S. Epling, N. Currier, H.Y. Chen, H. Hess, and

D. Lafyatis, "Mechanisms of Sulfur Poisoning of NOx Adsorber Materials", in Combustion and Emission Control for Advanced CIDI Engines: 2004 Annual Progress Report, pp. 184-189.

6. D.H. Kim, Y.-H. Chin, J.-H. Kwak, J. Szanyi, and C.H.F. Peden, "Changes in Ba Phases in BaO/Al_2O_3 upon Thermal Aging and H_2O Treatment", Catalysis Letters, 105 (2005) 259.
7. A. Yezerets, N. Currier, D.H. Kim, H. Eadler, W.S. Epling, and C.H.F. Peden, "Differential Kinetic Analysis of Diesel Particulate Matter (soot) Oxidation by Oxygen Using a Step–Response Technique", Appl. Catal. B, 61 (2005) 120.

References

1. Epling, W.S.; Campbell, L.E.; Yezerets, A.; Currier, N.W.; Parks, J.E. *Catal. Rev.–Sci. Eng.* 2004, 46, 163.
2. Bartholomew, C.H. *Appl. Catal. A* 2001, 212, 17.
3. Engstrom, P.; Amberntsson, A.; Skoglundh, M.; Fridell, E.; Smedler, G. *Appl. Catal. B* 1999, 22, L241.
4. Szanyi, J.; Kwak, J.H.; Kim, D.H.; Burton, S.D.; Peden, C.H.F. *J. Phys. Chem. B* 2005, 107, 27.

II.B.3 Dedicated and Regenerable Sulfur Traps for Diesel Engine Control

David King (Primary Contact), Liyu Li
Pacific Northwest National Laboratory
P.O. Box 999
Richland, WA 99352

DOE Technology Development Manager: Ken Howden

CRADA Project with Caterpillar Inc.

Objectives

- Develop a low-cost dedicated sulfur oxide (SOx) trap with capacity exceeding 40 wt% (SO_2 basis) that is capable of operating at temperatures of 200°C and below.
- Develop a regenerable SOx trap able to remove 99% of SOx from diesel exhaust and capable of operating under lean-rich cycling conditions as defined for the downstream NOx trap.

Approach

- Modify cryptomelane SOx absorbent with silver to improve low-temperature performance and test over a range of temperatures and compositions.
- Develop a lower-capacity but fully regenerable SOx trap by improving current copper-based adsorbents and demonstrate performance at bench scale.
- Prepare sufficient materials (both types) to washcoat onto monoliths for more realistic materials testing.

Accomplishments

- A novel silver-modified cryptomelane material (silver hollandite) was synthesized and characterized. The preparation method, which allowed access to a previously unobtainable material, was novel and efficient and resulted in a patent application being filed.
- Silver hollandite was tested and was shown to have a breakthrough capacity (SOx out = 0.01 x SOx in) of 8.7 wt% at 150°C and 27 wt% at 200°C, far better than other reported dedicated SOx absorbers.
- A novel regenerable SOx adsorber was developed. The composition, which has been filed for patent application, is based on a non-precious metal on an inert silica support. It is capable of operation under the lean-rich cycling required for NOx traps with at least 90% SOx removal over the temperature range 250-550°C.
- Sufficient quantities of cryptomelane and the regenerable adsorber were synthesized and shipped for washcoating on monoliths for larger-scale testing.

Future Directions

- The PNNL portion of the Cooperative Research and Development Agreement (CRADA) project reached completion in September 2005 and no additional development work is planned.

Introduction

The emission of NOx from on-road diesel trucks is an important environmental problem. Major efforts are underway to reduce these emissions through the implementation of NOx conversion devices such as regenerable NOx traps, which store NOx as surface nitrates. Sulfur oxides (primarily SO_2) that are present in the diesel exhaust will gradually decrease the effectiveness of NOx traps. SO_2 is oxidized to SO_3 over the NOx trap catalyst, and SO_3 reacts to form sulfates that block NOx

adsorption sites. The sulfates are not removed during the rich gas regeneration period that converts adsorbed nitrates to N_2, leading to the need for a high-temperature desulfation step. This results in a gradual degradation of the NO_x trap over the course of many cycles.

An approach to improving NOx trap longevity is to develop a reliable SOx trap that can be placed upstream of the NOx trap. The SOx trap may comprise a high-capacity adsorbent that can be replaced at regular intervals during engine maintenance, or it may operate as a trap that is regenerated during operation on the vehicle. In either case, the trap must be capable of operating effectively in an environment where it is exposed to the same lean/rich cycling of input gases as is utilized to operate the NOx trap.

Approach

We have previously identified a promising class of stoichiometric absorbents based on manganese oxide octahedral molecular sieves (OMSs), the most effective material of this type being cryptomelane. One of the expressed needs was to improve the low-temperature performance of this material so that a reasonable capacity could be obtained at temperatures as low as 150°C. Our approach was to modify this material by varying cation compositions (standard cryptomelane comprises K^+ cations). We expected that specific cations might improve the low-temperature oxidation function necessary to oxidize SO_2 to SO_3, allowing trapping of the original SO_2 as a manganese sulfate.

For the regenerable SOx trap we examined the current best materials, which appeared to be alumina-supported copper oxide. We discovered, however, that this composition is unsatisfactory as a regenerable trap because regeneration of the $CuSO_4$ under rich conditions competed with reduction of CuO to Cu metal. As a result, it became virtually impossible to fully regenerate the trap during the short rich cycle. In addition, formation of aluminum sulfate, $Al_2(SO_4)_3$, provided a storage medium for SOx that could not be reliably controlled under elevated temperature operation. For this reason, we decided to examine alternate metal-support combinations as candidates for the fast regenerable SOx adsorbents.

Results

Low-temperature SO_2 absorption by Ag-hollandite dedicated trap

Previously we reported that cryptomelane is an excellent SOx absorbent for diesel engine emission control [1]. At 325°C and 8000 hr^{-1} gas hourly space velocity (GHSV), it absorbs more than 70 wt% SO_2 by oxidizing SO_2 to SO_3 and forming $MnSO_4$. However, at low temperature, its SOx capacity is greatly reduced. We examined modifications to the cryptomelane via ion exchange in an effort to increase the low-temperature oxidation capacity. Silver is known to provide oxidation activity, but ion exchanging cryptomelane with Ag^+ was found to produce an unstable material. However, we developed a novel method to introduce silver cations into the structure by treatment in a silver nitrate melt, producing a material that had been previously described as silver hollandite. Previous efforts to make such a material required extreme conditions and long synthesis times and resulted in a very low-surface-area material that would prove ineffective as an absorbent [2]. The new synthesis method that we discovered resulted in a material having much higher surface area [3]. We prepared two samples, (A) and (B), which differed in their method of preparation (time and temperature of exposure to $AgNO_3$). We examined these silver hollandite samples for SOx absorption at low temperatures. Table 1 compares the low-temperature SO_2 absorption performance of silver hollandite and cryptomelane. Compared to cryptomelane, Ag-hollandite shows much higher SO_2 capacity at low temperatures. Silver hollandite B showed the best performance at low temperatures, although at temperatures 250°C and above, sample A performed slightly better. However, at 325°C and

Table 1. SO_2 Breakthrough Capacity of Ag-Hollandites and Other Absorbents

absorbent	150°C	200°C	250°C	325°C
cryptomelane	1.54	1.60	2.90	63.85
Ag-hollandite B	8.75	26.84	33.52	42.5
Ag-hollandite A	2.20	5.20	38.1	43.3

Feed: 10 ppm SO_2 in air unless specified, GHSV: 60 K hr^{-1}.

Breakthrough capacity: defined as the point where SO_2 out exceeded 100 ppb

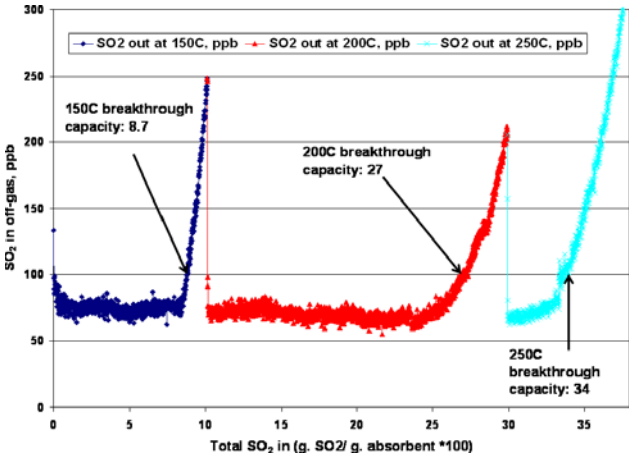

Figure 1. SO_2 Absorption on Ag-Hollandite B at Different Temperatures. Feed gas: 10 ppm SO_2 in air, 60,000 hr^{-1} GHSV. After SO_2 breakthrough at low temperature, the same absorbent was tested at a higher temperature. Breakthrough capacity (100 x g. SO_2/g. absorbent) is defined as the point where SO_2 out exceeded 100 ppb.

above, cryptomelane shows much higher SOx capacity. Figure 1 shows the SO_2 absorption curve for Ag-hollandite B. The breakthrough capacities could be obtained at 150, 200, and 250°C in a single experiment. Following SO_2 absorption by Ag-hollandite, x-ray diffraction indicated that $MnSO_4$ is produced along with Ag_2SO_4. To our knowledge, Ag-hollandite is the best low-temperature SO_2 absorbent that has been described in the literature. Combining Ag-hollandite with cryptomelane, a high-capacity SO_x trap that is active at both low temperatures (~150°C) and high temperatures (~550°C) can be developed.

Development of a regenerable SOx trap

The performance of a simple adsorbent, 5 wt% metal (M) on fumed SiO_2, was studied in this work. Figure 2 shows sulfation/desulfation test results (not under lean-rich cycling conditions). The purpose of the test was to determine the SO_2 adsorption performance under lean conditions and the SO_2 desorption performance under rich conditions. The test was carried out as follows: first, the adsorbent was heated from room temperature to 560°C at 10°C/min in simulated lean exhaust feed gas at 100K hr^{-1} GHSV, during which SO_2 adsorption occurred (sulfation test). After cooling in air to 50°C, the sample was heated to 560°C at 10°C/min in

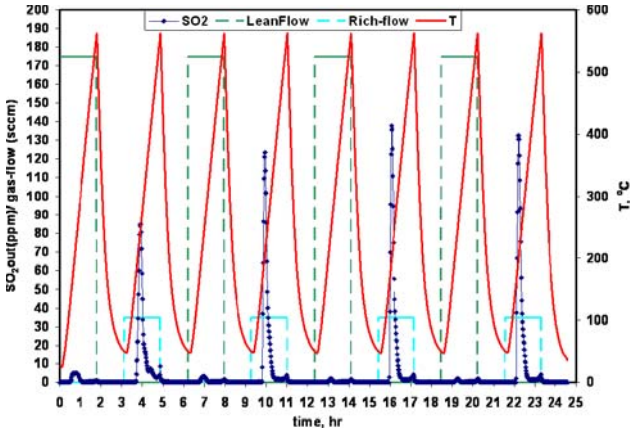

Figure 2a. A Sulfation/Desulfation Test Result for Sample 5wt%M-SiO_2

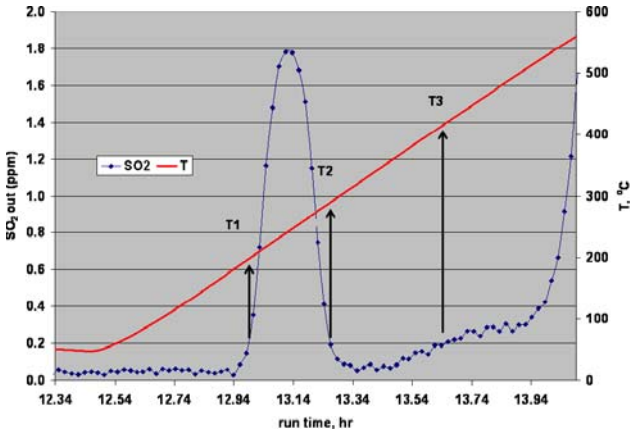

Figure 2b. A Typical Sulfation Step of the Sulfation/ Desulfation Test

simulated rich exhaust feed at 20K hr^{-1} GHSV, during which SO_2 desorbed (desulfation test). After cooling again to 50°C in air, the sample was heated to 560°C in lean feed for a second sulfation test, and then a second desulfation followed after first cooling down to 50°C. Figure 2a shows the results of four such sulfation/desulfation cycles, showing that by the second cycle, the system had reached a reproducible steady-state performance. During the test, SO_2 concentration in the off-gas was measured using a gas chromatograph equipped with a sulfur chemiluminescent detector system. From each sulfation test, SO_2 breakthrough (defined at 200 ppb SO_2) capacities at three different temperatures can be obtained, as shown in Figure 2b. The initial low-temperature capacity at T1 can be calculated (~200°C) based on feed SO_2 concentration and time. Above T1, the SO_2 concentration in the exit stream exceeds 200 ppb. However, as the temperature

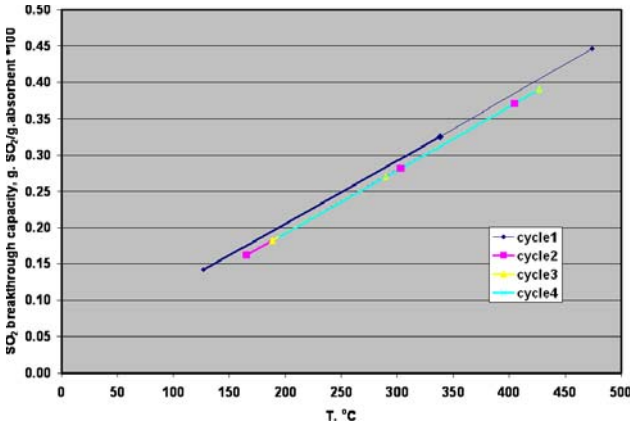

Figure 2c. Temperature Effect of SO_2 Breakthrough Capacities during Different Sulfation Cycles

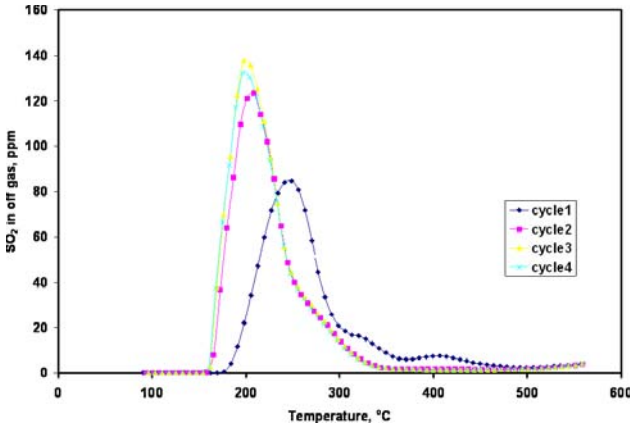

Figure 2d. Temperature Effect of SO_2 Desorption on Sulfated Adsorbent during Different Desulfation Cycles

continues to ramp upward, the SO_2 concentration first increases and then decreases until SO_2 in the effluent is again at 200 ppb (at T2). The capacity at T2 can again be calculated based on time on stream and SO_2 concentration in the off gas. Eventually, at T3 the SO_2 in the effluent once again reaches 200 ppb and the capacity at that temperature can again be calculated. From each desulfation test, a temperature-programmed reduction curve can be obtained. Figures 2c and 2d summarize SO_2 adsorption and desorption performance from the four sulfation-desulfation cycles. The SO_2 adsorption (sulfation) capacity as a function of temperature, shown in Figure 2c, appears to behave linearly, allowing one to estimate the total capacity at any operating temperature over a broad temperature range from about 200°C to 450°C. The results shown in Figure 2d indicate that once steady-state operation of the adsorbent is achieved (starting at the second cycle), full desulfation can be achieved at approximately 300°C and higher. Based on the sulfur balance, more than 90% of sulfur that is adsorbed during the sulfation step is removed during the subsequent desulfation step. This is consistent with a constant sulfation performance of the adsorbent after the first cycle. The performance of this 5 wt% M on SiO_2 adsorbent is much better than that of Cu-based materials in terms of low-temperature SO_2 adsorption and desorption.

The M-SiO_2 sample was further tested under lean-rich cycles similar to those proposed for NOx traps at different temperatures. Gas compositions for the lean and rich cycles are provided in Table 2. The tests were carried out at a temperature range of 200°C to 550°C with cycling with 40 sec rich feed at 20K hr^{-1} GHSV and 4 min lean feed at 100K hr^{-1} GHSV, for a total test duration of 32 hr (4 hr at each temperature). During the lean cycles carried out at temperature higher than 250°C, more than 90% SO_2 was adsorbed as measured by gas chromatograph (GC), and during the short period of rich cycles, a large amount of SO_2 was released. No H_2S, COS or other sulfur species were measured during the rich cycles based on mass spectrometric measurement. Our system cannot accurately quantify the SO_2 concentration released during rich cycles since each GC measurement needs about 1 minute and each rich cycle only lasts 40 seconds. However, based on the combined information from the GC and mass spectrograph (MS), the maximum SO_2 concentration eluted during the rich cycles is more than 100 ppm, and virtually all the sulfur is desorbed as SO_2. Under

Table 2. Composition of Simulated Diesel Engine Lean and Rich Exhaust Used in the Study

Simulated Exhaust	CO	CO_2	C_3H_6	H_2	SO_2	O_2	NO_2	NO	N_2
Lean	–	5%	–	–	5.15 ppm	12%	20 ppm	180 ppm	Balance
Rich	2%	12.5%	333 ppm	2%	–	–	–	–	Balance

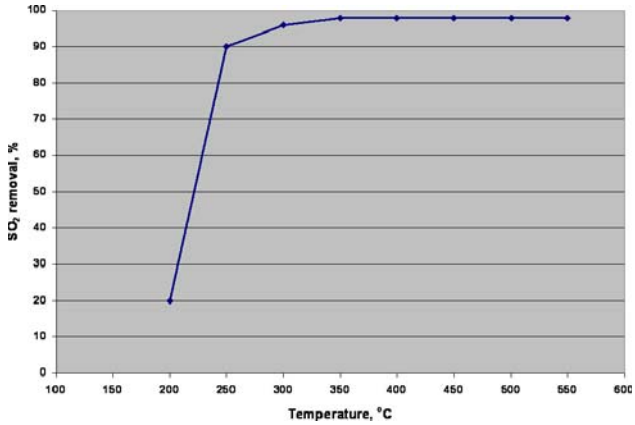

Figure 3. SO_2 Removal Efficiency during Lean Cycles at Different Temperatures

the tested conditions, this adsorbent performed flawlessly for 32 hours (411 lean-rich cycles) without showing any performance change, i.e., stable SO_2 removal was observed during the lean cycles. This indicates that the adsorbent is mostly if not completely regenerated during the rich cycles. Figure 3 summarizes the SO_2 removal efficiency during lean cycles at different temperatures.

Conclusions

- Silver hollandite, a modification to the previously developed cryptomelane dedicated SOx trap based on ion exchanging Ag+ cations into the structure, has demonstrated superior low-temperature breakthrough absorption capacity. A novel method to prepare this material was developed and a patent applied for.
- A combination of silver hollandite and cryptomelane produces a SOx adsorber that possesses the best of both low-temperature and high-temperature capacity.
- A silica-supported metal, 5%M/SiO_2, has been developed that shows acceptable capacity toward SO_2 under lean feed conditions.
- The 5%M/SiO_2 adsorber has demonstrated excellent performance under lean-rich cycling tests over the temperature range 250-550°C. A patent application for use of this material has been filed.

FY 2005 Publications/Presentations

1. Liyu Li and David L. King, Cryptomelane as High-Capacity Sulfur Dioxide Adsorbent for Diesel Emission Control: A Stability Study. Ind. Eng. Chem. Res. (2005) 44, 7388-7397.
2. Liyu Li and David L. King, Synthesis and Characterization of Silver Hollandite and its Application in Emission Control. Chemistry of Materials (2005) 17(17), 4335-4343.
3. Liyu Li and David L. King, High Capacity Sulfur Dioxide Adsorbents for Diesel Emissions Control. Ind. Eng. Chem. Res. (2005) *44*, 168-177.
4. David L. King and Liyu Li, High Capacity Sulfur Dioxide Absorbents for Diesel Engine Emissions Control. Presented at the 19th North American Catalysis Society Meeting, Philadelphia, PA, on May 25, 2005.
5. David L. King and Liyu Li, High Capacity SOx Adsorbents for Diesel Engine Emissions Control Based on Octahedral Molecular Sieve Compositions. Presented by D.L. King (Invited Speaker) at the 2005 Meeting of the Pacific Coast Catalysis Society, Berkeley, CA, on March 11, 2005.
6. Liyu Li and David L. King, Ag-Hollandite: Low Temperature SOx Absorber and Oxidation Catalyst for Emission Control. Presented by L. Li at the Department of Energy National Laboratory Advanced Combustion Engine R&D Merit Review and Peer Evaluation, Argonne, IL, on April 19, 2005.
7. Liyu Li and David L. King, Synthesis and Characterization of Silver Hollandite and its Application in Emission Control. Presented by L. Li at the 230th American Chemical Society Meeting & Exposition, Washington, DC, on August 31, 2005.
8. Liyu Li and David L. King, Cryptomelane as High Capacity Sulfur Dioxide Absorbent for Diesel Emission Control. Presented by L. Li at the 230th American Chemical Society Meeting & Exposition, Washington, DC, on September 1, 2005.

References

1. Li, L.Y.; King, D.L. *Ind. Eng. Chem. Res.* 2005, *44*, 168-177.
2. Chang, F.M.; Jansen, M. *Angew. Chem. Int. Ed. Engl.* 1984, *23(11)*, 906-907.
3. Li, L.Y.; King, D.L. *Chemistry of Materials* 2005, *17(17)*, 4335-4343.

Patents

1. An international patent (WO 2005/077498 A1) titled "Sulfur Oxide Adsorbents and Emissions Control" was awarded to David King and LI Liyu of PNNL on August 25, 2005.

II.B.4 Characterizing Lean NOx Trap Regeneration and Desulfation

Shean Huff (Primary Contact), Brian West, James Parks, Matt Swartz
Oak Ridge National Laboratory
2360 Cherahala Boulevard
Knoxville, TN 37932

DOE Technology Development Manager: Ken Howden

Objectives

- Establish a relationship between exhaust species and various lean NOx trap (LNT) regeneration strategies
- Characterize effectiveness of in-cylinder regeneration strategies
- Develop stronger link between bench and full-scale system evaluations
  - Provide data through Cross-Cut Lean Exhaust Emissions Reduction Simulations (CLEERS) to improve models to guide engine research

Approach

- Characterize H_2, CO, and hydrocarbons (HCs) generated by the engine
  - Use Fourier transform infrared (FTIR), gas chromatograph/mass spectrometer (GC/MS), and spatially resolved capillary inlet mass spectrometry (SpaciMS) to characterize engine strategies
- Characterize candidate LNTs for performance and degradation
  - Correlate various reductants with catalyst performance
- Develop and execute rapid sulfation/desulfation experiments
- Develop experiments for bench-scale work to further characterize LNT monoliths, wafers, and/or powders

Accomplishments

- Presented reductant chemistry paper at the SAE Powertrain & Fluid Systems Conference [1]
- Conducted detailed particulate matter (PM) investigation using laser-induced incandescence (LII)
  - Paper presented at SAE Congress [2]
- Conducted reductant utilization study
  - *in-situ* measurements
  - Varied: strategy, lean loading period, minimum air-fuel ratio (AFR), catalyst configuration
- Continued to collaborate through CLEERS
- Investigated nitrogen selectivity (ammonia formation)
- Characterized low-temperature combustion (LTC)-based regeneration
- Investigated temperature effects
- Developed rapid sulfation protocol
- Developed improved desulfation control
  - Strategies for stable control of 550-850°C LNT temperature

Future Directions

- Further investigate temperature dependence of strategy effectiveness (200, 300, and 400°C)
- Extend study to model other catalysts supplied by the Manufacturers of Emission Controls Association (MECA)

- Investigate potential for improved NOx conversion of LTC regeneration while targeting minimal fuel penalty
- Improve understanding of desulfation phenomena through engine-based rapid sulfation/desulfation experiments
- Continue to share results and coordinate research plans through CLEERS LNT focus group and other industry contacts

Introduction

As part of the Department of Energy's strategy to reduce imported petroleum and enhance energy security, the Office of FreedomCAR and Vehicle Technologies has been researching enabling technologies for more efficient diesel engines. NOx emissions from diesel engines are very problematic, and the U.S. Environmental Protection Agency (EPA) emissions regulations require ~90% reduction in NOx from light- and heavy-duty diesel engines in the 2004-2010 timeframe. An active research and development focus for lean burn NOx control is in the area of LNT catalysts. LNT catalysts adsorb NOx very efficiently in the form of a nitrate during lean operation, but must be regenerated periodically by way of a momentary exposure to a fuel-rich environment. This rich excursion causes the NOx to desorb and then be converted by more conventional three-way catalysis to N_2. The momentary fuel-rich environment in the exhaust can be created by injecting excess fuel into the cylinder or exhaust and/or throttling the intake air and/or increasing the amount of exhaust gas recirculation (EGR). The controls methodology for LNTs is very complex, and there is limited understanding of the regeneration mechanisms. NOx regeneration is normally a 2-4 second event and must be completed approximately every 30-90 seconds (duration and interval dependent on many factors; e.g., load, speed, and temperature).

While LNTs are effective at adsorbing NOx, they also have a high affinity for sulfur. As such, sulfur from the fuel and possibly engine lubricant (as SO_2) can adsorb to NOx adsorbent sites (as sulfates). Similar to NOx regeneration, sulfur removal (desulfation) also requires rich operation, but for several minutes, at much higher temperatures. Desulfation intervals are much longer, on the order of hundreds or thousands of miles, but the conditions are more difficult to achieve and are potentially harmful to the catalyst function. Nonetheless, desulfation must be accomplished periodically to maintain effective NOx performance. There is much to be learned with regard to LNT performance, durability, and sulfur tolerance.

Different strategies for introducing the excess fuel for regeneration can produce a wide variety of hydrocarbons and other species. One focus of this work is to examine the effectiveness of various regeneration strategies in light of the species formed and the LNT formulation. Another focus is to examine the desulfation process and examine catalyst performance after numerous sulfation/desulfation cycles. Both regeneration and desulfation will be studied using advanced diagnostic tools.

Approach

A 1.7-L Mercedes common rail engine and motoring dynamometer have been dedicated to this activity. The engine is equipped with an electronic engine control system that provides full bypass of the original equipment engine controller. The controller is capable of monitoring and controlling all the electronically controlled parameters associated with the engine (i.e., fuel injection timing/duration/number of injections, fuel rail pressure, turbo wastegate opening, electronic throttle, and electronic EGR).

Three regeneration strategies have been studied with the goal of introducing a broad range of species to the LNT catalyst. Two of the strategies use throttling to reduce the intake air flow and reduce the exhaust AFR; they then introduce excess fuel into the cylinder to produce a rich AFR. The first of these two strategies applies the excess fuel by extending the main fuel pulse and delaying it in crank angle time (delayed and extended main or DEM). The second strategy introduces the excess fuel in a late cycle post injection at 80 degrees after top dead center (ATDC) (Post80). In addition to these two

strategies, a third strategy uses EGR in place of throttling to reduce the intake air flow and reduce the exhaust AFR. The EGR is increased to approximately 55% while the pilot injection is disabled and the main injection timing is advanced to stabilize the combustion. These changes drive the engine into an advanced combustion regime referred to as low-temperature combustion (LTC). LTC is characterized by simultaneous low NOx and low PM emissions. Once the engine is operating in the LTC regime, a nominal amount of excess fuel is applied to the main fuel pulse to produce a rich AFR. These strategies are then used to study catalysts under quasi-steady conditions, that is, steady load and speed but with periodic regeneration.

Accomplishments for FY 2005 can be categorized into four main areas. The first area of research involved studying factors controlling the nitrogen selectivity, or how to promote the LNT to selectively reduce the NOx to N_2 versus other harmful nitrogen compounds such as ammonia (NH_3) or nitrous oxide (N_2O). The second area of research involved characterizing the effectiveness of the LTC regeneration strategy and comparing it to both the DEM and Post80 strategies. Thirdly, LNT temperature effects on NOx performance were studied. And finally, a rapid sulfation and desulfation protocol was developed.

Advanced tools such as H_2-SpaciMS and GC/MS are being used to characterize the species produced in the engine or in upstream catalysts. The H_2-SpaciMS is being used for both in-pipe and in-situ measurements within the catalyst monoliths. In addition, catalysts and exhaust species will be characterized after rapid sulfation and during desulfation. LNT catalysts have been provided by some MECA members. "Model" catalysts will also be characterized.

Finally, bench-scale work will be used to further characterize LNT monoliths, wafers, and/or powders using our bench-scale reactor and the diffuse reflectance infrared Fourier transform spectroscopy (DRIFTS) reactor. Results and characteristics of the engine experiments will be used to help define more meaningful bench-scale studies. In some cases, the exact same catalyst formulation being studied on the engine stand is also being examined in the bench studies.

Results

Summary of Nitrogen Selectivity Study

It has been generally observed that the duration of the rich regeneration greatly affects the production of ammonia. This phenomenon has been studied on the engine by performing sweeps of the rich duration during periodic regenerations. Rich durations between one second and five seconds were studied. Figure 1 shows bench flow data for an extended LNT sorption and regeneration cycle that supports the engine findings. A theory by Lesage et al. [3] proposes that isocyanate (NCO) is an intermediate species that plays a role in NH_3 formation; this theory also proposes that in the presence of oxygen (O_2), isocyanate does not produce ammonia. This hypothesis led to experiments in which the standard three-second rich duration was pulsed in one-second intervals with a one-second lean separation between each pulse. This strategy resulted in lower levels of NH_3 and slightly improved NOx reduction. Figure 2 shows that the LNT is being purged with O_2 during the lean separation compared to the standard three-second rich pulse, where the O_2 concentration goes to zero. This data supports the isocyanate-pathway model for NH_3 production, in that NH_3 is produced in the complete absence of O_2, but not when O_2 is present during regeneration. This research has been published in SAE 2005-01-3876 [4].

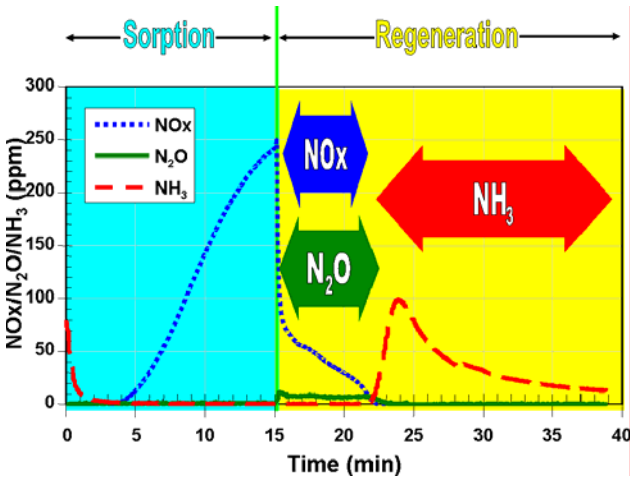

Figure 1. Lean NOx Trap Cycle at 300ºC with Low Reductant Mass Flow during Regeneration to Demonstrate the Sequence of NOx Reduction, N_2O and NH_3 Formation, and Reductant (CO) Breakthrough during Regeneration

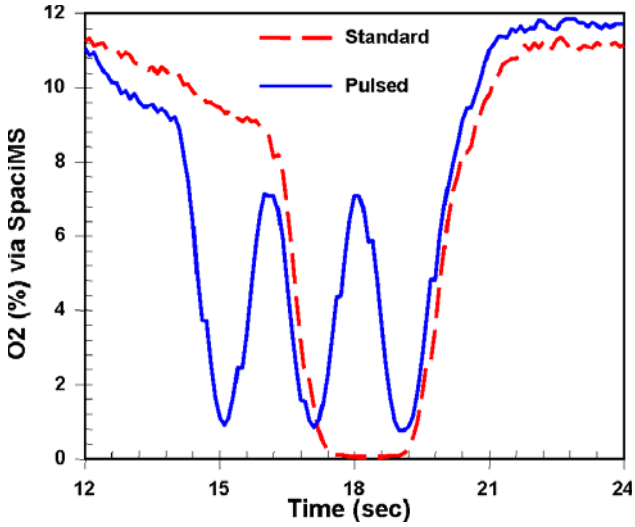

Figure 2. O_2 Measured at the Tailpipe Position for the Standard and Pulsed Lean-Rich Strategies

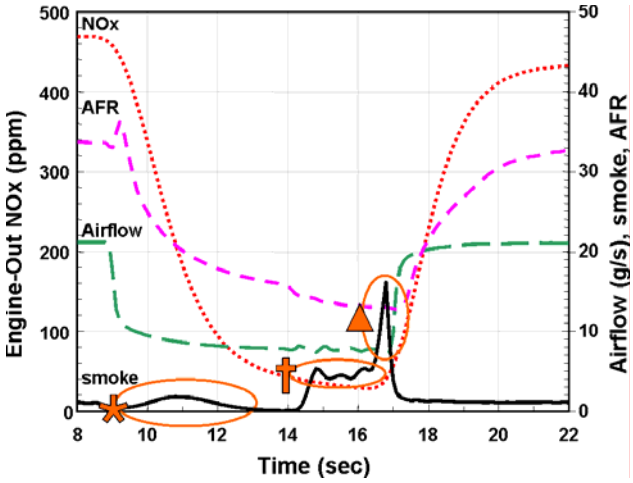

Figure 3. Real-Time NOx, Mass Air Rate, AFR, and Smoke for LTC Strategy

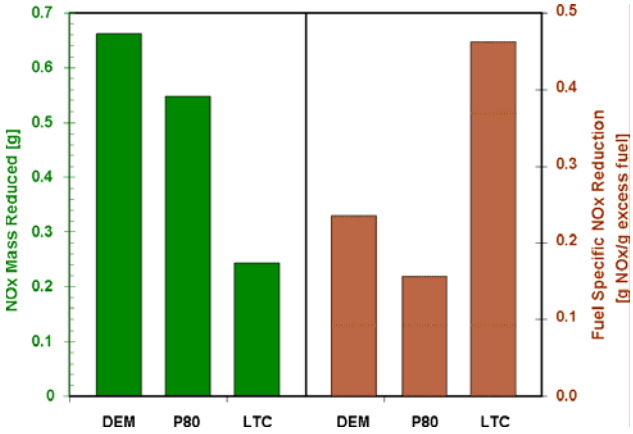

Figure 4. Total NOx Reduced and Fuel-Specific NOx Reduction for DEM, P80, and LTC Regeneration

Summary of LTC Regeneration Characterization

As mentioned earlier, LTC is characterized by low engine-out NOx and PM. It is also characterized by low O_2 content, which enables the obtainment of a rich AFR without throttling, and a diverse reductant pool similar to other strategies. For these reasons, LTC is being investigated as an LNT regeneration strategy.

Figure 3 highlights the characteristics of the LTC strategy. Note that as the EGR was increased, the NOx level dropped dramatically. Also note the sharp decrease in airflow as the EGR valve was opened quickly. The corresponding decrease in AFR associated with EGR was much slower, as the lean exhaust must recirculate through multiple cycles before having a significant impact on intake O_2 concentration and therefore the exhaust AFR. As EGR rate increases, smoke begins to increase and then decreases as the engine enters into the LTC regime (✱). A nominal fueling increase is added to quickly transition into the rich regime for regeneration of the LNT, resulting in a small step change in the smoke level (†). Finally, as the EGR valve is closed and normal fueling is restored, the data shows a small spike in the smoke at the end of the regeneration (▲).

Figure 4 shows the mass of NOx reduced per regeneration cycle for each strategy. This data shows that the DEM strategy reduces the largest NOx mass, while LTC reduces the least. This trend directly follows the trend of H_2 production. This result supports the conclusion that H_2 availability controls NOx reduction [1].

Figure 4 also shows the fuel-specific NOx reduction (grams of NOx reduced per gram of excess fuel required to regenerate). Note that while the LTC strategy was the least effective for NOx reduction, it is dramatically better than both DEM and P80 on a fuel-specific basis. It is important to note that none of these strategies have been tuned for minimum catalyst regeneration fuel penalty, torque stability, or maximum NOx reduction. Despite the poorer initial performance of LTC, the superior fuel-specific NOx reduction of the LTC strategy indicated tremendous

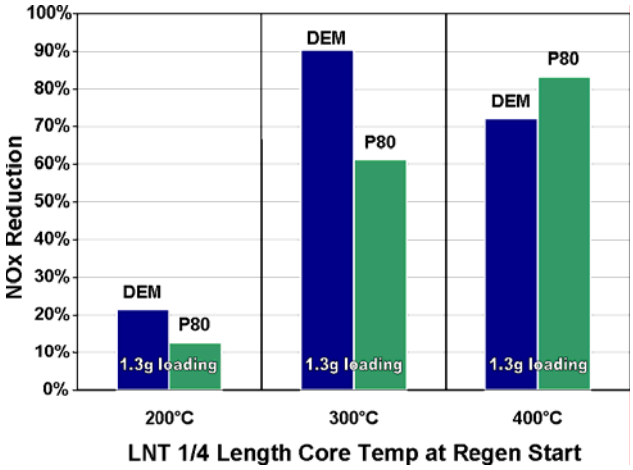

Figure 5. NOx Reduction Efficiency vs. Temperature for DEM with Constant NOx Loading

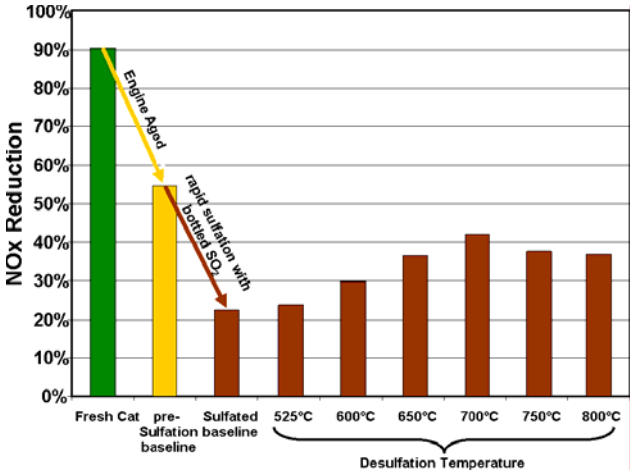

Figure 6. NOx Reduction Efficiency vs. Catalyst State for DEM at 300°C

room for improvement in NOx reduction while possibly maintaining a low fuel penalty. For more detail on the LTC regeneration study, please see references 5 and 6.

Summary of Temperature Effects

A study was performed on a fresh catalyst at three different temperatures, including 200°C, 300°C, and 400°C as defined by the ¼ length core temperature at the start of each regeneration. The strategies were engineered to have equivalent reductants at all temperatures.

Figure 5 shows the results of the study with the strategies being engineered for constant NOx loading between regenerations. The data shows that DEM performance is best at 300°C and better than Post80 at both 200°C and 300°C. Conversely, Post80 performance is best at 400°C and better than DEM at that temperature. However, the 400°C results are clouded by thermal desorption issues. Measurements of exhaust H_2 levels revealed that for the 400°C DEM case, a large portion of the H_2 was consumed across the diesel oxidation catalyst. In fact, the H_2 level at the inlet of the LNT for the 400°C DEM was less than that for Post80. This result again supports the conclusion that H_2 availability controls NOx reduction [1].

Summary of Sulfation/Desulfation Development

LNTs store sulfates similar to nitrates, requiring periodic desulfations to remove the sulfur. It is challenging to consistently desulfurize LNTs because sulfur removal efficiency and thermal degradation both increase with increasing temperature. Rapid sulfation allows for repeated desulfations in a controlled manner. The rapid sulfation was performed by bleeding a controlled flow of relatively high concentration sulfur dioxide into the exhaust stream during engine operation, which artificially poisoned the LNT in a repeatable manner.

Using an in-pipe fuel injection system and controlling engine speed, the catalyst temperature and AFR were tightly controlled when performing the desulfations. Highlighting the experimental progress, Figure 6 shows NOx reduction efficiency for multiple catalyst states, including a fresh-degreened state, after more than 1000 hours of engine aging with 15 ppm sulfur diesel fuel, after a rapid sulfation, and following repeated desulfations at successively higher temperatures. These desulfations were consistent and repeatable using the described method. This data indicates that above 700°C desulfation temperature, the thermal degradation begins to offset improvement due to sulfur removal for this catalyst formulation.

Conclusions

Strategies for in-cylinder regeneration have been developed for studying reductant chemistry effects on LNTs. Notable conclusions are the following:

- NH_3 can be formed by LNTs during regeneration, and regeneration details

dramatically affect production rate. Our measurements show that O_2 is important, as well as the length of the rich period.

- Isocyanate mechanism appears to have validity, and controls to allow isocyanate combustion on catalyst via O_2 purge appear feasible.
- LTC regeneration produces PM levels less than those of typical lean/EGR operation.
- Demonstrated low fuel requirement suggests LTC strategy may be more fuel efficient means of LNT regeneration compared to DEM/Post80.
- DEM has better NOx reduction efficiency at 200°C and 300°C.
- Post80 has better NOx reduction efficiency at 400°C.
- Desulfation using in-pipe injection is more stable and controllable than in-cylinder techniques.
- Desulfation with in-pipe strategy shows that bulk of sulfur is released between 600°C and 700°C.

FY 2005 Publications/Presentations

1. Brian West, Shean Huff, James Parks, Sam Lewis, Jae-Soon Choi, William Partridge, and John Storey, "Assessing Reductant Chemistry During In-Cylinder Regeneration of Diesel Lean NOx Traps," *Society of Automotive Engineers Technical Series* 2004-01-3023 (2004).
2. Peter Witze, Shean Huff, John Storey, and Brian West, "Time-Resolved Laser-Induced Incandescence Measurements of Particulate Emissions During Enrichment for Diesel Lean NOx Trap Regeneration," *Society of Automotive Engineers Technical Series* 2005-01-0186 (2005).
3. Shean Huff, Brian West, Jim Parks, Matt Swartz, Johney Green, and Ron Graves, "Combining Low-Temperature Combustion with Lean-NOx Trap Yields Progress Toward Targets of Efficient NOx Control for Diesels," 2005 Diesel Engine Emissions Reduction Conference, August 2005.
4. Shean Huff, Brian West, Jim Parks, Matt Swartz, Johney Green, and Ron Graves, "Fuel Efficient Diesel Engine Emissions Controls," Oak Ridge National Laboratory - Engineering Science and Technology Division Advisory Committee, October 2005.
5. Jim Parks, Shean Huff, Josh Pihl, Jae-Soon Choi, and Brian West, "Nitrogen Selectivity in Lean NOx Trap Catalysis with Diesel Engine In-Cylinder Regeneration," *Society of Automotive Engineers Technical Series* 2005-01-3876 (2005).
6. Shean Huff, Brian West, Jim Parks, Matt Swartz, Johney Green, and Ron Graves, ìIn-Cylinder Regeneration of Lean NOx Trap Catalysts Using Low Temperature Combustion,î*Society of Automotive Engineers Technical Series* (in press for April 2006 SAE Congress).

References

1. Brian West, Shean Huff, James Parks, Sam Lewis, Jae-Soon Choi, William Partridge, and John Storey, "Assessing Reductant Chemistry During In-Cylinder Regeneration of Diesel Lean NOx Traps," *Society of Automotive Engineers Technical Series* 2004-01-3023 (2004).
2. Peter Witze, Shean Huff, John Storey, and Brian West, "Time-Resolved Laser-Induced Incandescence Measurements of Particulate Emissions During Enrichment for Diesel Lean NOx Trap Regeneration," *Society of Automotive Engineers Technical Series* 2005-01-0186 (2005).
3. T. Lesage, C. Verrier, P. Bazin, J. Saussey, and M. Daturi, "Studying the NOx-Trap Mechanism over a Pt-Rh/Ba/Al_2O_3 Catalyst by Operando FT-IR Spectroscopy," *Phys. Chem. Chem. Phys.*, **5**, 4435-4440 (2003).
4. Jim Parks, Shean Huff, Josh Pihl, Jae-Soon Choi, and Brian West, "Nitrogen Selectivity in Lean NOx Trap Catalysis with Diesel Engine In-Cylinder Regeneration," *Society of Automotive Engineers Technical Series* 2005-01-3876 (2005).
5. Shean Huff, Brian West, Jim Parks, Matt Swartz, Johney Green, and Ron Graves, "Combining Low-Temperature Combustion with Lean-NOx Trap Yields Progress Toward Targets of Efficient NOx Control for Diesels," 2005 Diesel Engine Emissions Reduction Conference, August 2005.
6. Shean Huff, Brian West, Jim Parks, Matt Swartz, Johney Green, and Ron Graves, "In-Cylinder Regeneration of Lean NOx Trap Catalysts Using Low Temperature Combustion," *Society of Automotive Engineers Technical Series* (in press).

II.B.5 Advanced Engine/Aftertreatment System R&D

Brian H. West (Primary Contact), John Thomas
Oak Ridge National Laboratory
2360 Cherahala Boulevard
Knoxville, TN 37932

Cooperative Research and Development Agreement (CRADA) Partner:
International Truck and Engine Corporation, Alan Karkkainen

DOE Technology Development Manager: Ken Howden

Objectives

- Develop NOx adsorber regeneration and desulfation strategies for diesel aftertreatment systems (including diesel oxidation catalysts and diesel particle filters).
- Improve understanding of the role/fate of different exhaust hydrocarbons (HCs) in advanced diesel aftertreatment systems for several reductant delivery systems. International will focus on in-cylinder strategies while Oak Ridge National Laboratory (ORNL) will examine in-manifold and in-pipe strategies.
- Explore advanced combustion regimes and thermodynamic cycles using infinitely variable intake and exhaust valve timing.

Approach

- NOx adsorber regeneration strategies will be developed for several steady-state conditions. Electronic control of the intake throttle and the exhaust gas recirculation (EGR) valve will be used to lower air:fuel ratio prior to reductant (fuel) delivery in-pipe (into exhaust, upstream of catalysts).
- System performance will be measured for a variety of regeneration conditions and pure HC compound reductants.
- Over-expansion and trapped EGR on camless engine prototype will be investigated as means to improve efficiency and engine-out emissions.

Accomplishments

- Developed preliminary desulfation strategy at road-load condition.
- Evaluated iso-octane, toluene, and 1-pentene reductants to confirm rank order of various HC families in NOx adsorber regeneration.
- Removed camless engine prototype from vehicle for ORNL engine cell.

Future Directions

- Study NOx adsorber desulfation.
- Install camless engine at ORNL facility.
- Examine limits of over-expansion as means to higher efficiency.

Introduction

Heavy-duty emissions standards call for a 90% reduction in NOx and particulate matter (PM) emissions by 2010. These new regulations include certification at any and all engine operating conditions, wherein emissions may not exceed 150% of the emissions standard. This regulation is known as not-to-exceed (NTE) and includes steady operation at the rated load condition. The NOx

adsorber catalyst is a promising technology to help meet these stringent new NOx standards, but there are many open issues that must be resolved prior to commercialization. The (lean-burn) diesel engine is not designed to run fuel rich, but rich exhaust conditions are required to regenerate the NOx adsorber catalyst. With more flexible fueling systems and other advanced engine control schemes, engineers are devising means to run these engines rich during "normal" operation to regenerate NOx adsorber catalysts. However, the NTE points can include operating conditions at which rich engine operation could be detrimental to the engine and/or aftertreatment system. Producing rich exhaust conditions with diesel engines is challenging, as doing so can potentially cause engine durability problems, excessive fuel consumption, and excess PM, HC, and/or CO emissions.

Additionally, the NOx adsorber catalyst is very sensitive to sulfur in the exhaust; therefore, effective sulfur management schemes must be developed that will ensure full useful life of the aftertreatment systems. This CRADA project has focused on helping to resolve some of the problems and unknowns with NOx adsorber technology. Future efforts will continue to research advanced aftertreatment and combustion strategies via a unique camless engine prototype.

Approach and Results

International Truck and Engine has been pursuing engine-based (in-cylinder) approaches to NOx adsorber regeneration, while complementary experiments at ORNL have focused on in-pipe or in-exhaust (after turbo) fuel injection. ORNL has developed a PC-based controller for transient electronic control of EGR valve position, intake throttle position, and actuation of fuel injectors in the exhaust system. Aftertreatment systems consisting of different diesel oxidation catalysts in conjunction with a diesel particle filter and NOx adsorber have been evaluated under quasi-steady-state conditions while sampling for HC species at multiple locations in the exhaust system.

A catalyzed diesel particulate filter (CDPF) was installed just upstream of the NOx adsorber catalyst for all experiments, as shown in Figure 1. Previously reported studies examined fuel cracking upstream of the 14.0 liter NOx adsorber by using the CDPF alone and in conjunction with a 5.0 liter diesel oxidation catalyst (DOC). Gas chromatograph mass spectrometry (GC-MS) and Fourier transform infrared (FTIR) spectroscopy were used to speciate the hydrocarbons entering and exiting the NOx adsorber catalyst for the full-load, rated speed (FLRS) condition (450 ft-lb, 2300 RPM, ~600°C catalyst temperatures) and for a lower temperature "road load" condition (200 ft-lb, 1800 RPM, ~400°C catalyst temperatures). Previously reported results showed that at the FLRS condition, the presence of a DOC enhanced the NOx adsorber function with reductant (fuel) injection upstream of the DOC. GC-MS analysis of HC species entering and exiting the NOx adsorber showed high utilization of light alkenes, mono-aromatics, and poor utilization of branched alkanes. At this high temperature (600°C) condition, the fuel penalty for a given level of NOx reduction was reduced 10-20% with the DOC in place. Follow-on experiments at lower temperature were conducted, with the finding that the NOx reduction was better *without* the DOC. The improved performance was hypothesized to be attributed to the large swings in the NOx adsorber core temperature. The relatively cooler temperatures during the sorption phase are believed to enhance NOx storage, and higher temperatures during regeneration improve the chemical reduction process. Any enhancement of catalyst performance associated with cracking of fuel components was confounded by the differences in NOx adsorber temperature between the DOC and no-DOC cases.

In an attempt to better control the NOx adsorber temperature and the reductant chemistry at the road load condition, the experiment was modified to enable split or dual injection (Figure 1). This approach allows the bulk of the exotherm associated with oxygen depletion to occur in the DOC (from fuel injection before the DOC) and allows largely uncracked hydrocarbon compounds to be used in the regeneration (from injection downstream of the DOC). While the reductant must pass through the CDPF before entering the NOx adsorber, the age of this particular unit and previous GC-MS analysis of the HCs exiting the CDPF limited any concerns about its presence affecting the HCs injected at the DOC-out location. Moving or removing the CDPF

would affect exhaust backpressure, and increasing pipe length between the CDPF and NOx adsorber to enable a second injection at that location would have affected NOx adsorber temperatures. As such, the experiments were run with the setup shown in Figure 1. It is important to note that this split injection setup is intended as a means to improve understanding of the function of the DOC and NOx adsorber by better controlling the NOx adsorber temperature and reductant chemistry.

Split injection experiments have been conducted with ultra-low sulfur diesel fuel from BP/ARCO Petroleum (ECD-1) plus 3 pure HC compounds as reductants. The pure HCs were selected to represent a light alkene (1-pentene), a monoaromatic (toluene), and a branched alkane (2,2,4 trimethylpentane (iso-octane)). Figure 2 shows NOx conversion versus reductant delivery rate (as a fraction of engine fuel rate) for multiple experiments at the 1800 RPM, 200 ft-lb condition. Note that the ranking of the compounds confirms the previously reported findings from GC-MS analysis of HCs entering and exiting the NOx adsorber. Pentene is the most effective HC reductant, followed by toluene and finally iso-octane. Considering the chemical reduction potential for each reductant ensures a fair comparison of reductant effectiveness. Table 1 shows selected properties of the four reductants. Chemical reduction potential is defined as the number of grams of oxygen required for complete (stoichiometric) oxidation of 1 gram of the reductant. Normalized to diesel fuel, note that toluene has a lower reduction potential, meaning that a larger mass of toluene would be required to consume the same mass of oxygen than a given mass of diesel fuel. The inverse of this reduction potential is also shown, the stoichiometric mass of reductant consumed (oxidized) by 1 gram of oxygen. As an example, a 5% diesel fuel penalty would be comparable to a 5.4% penalty using toluene. Conversely, slightly smaller masses of pentene and iso-octane would be

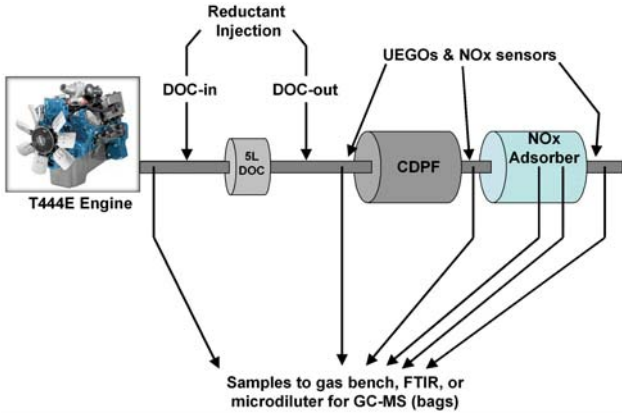

Figure 1. Exhaust Schematic for Engine-Based NOx Adsorber Experiments

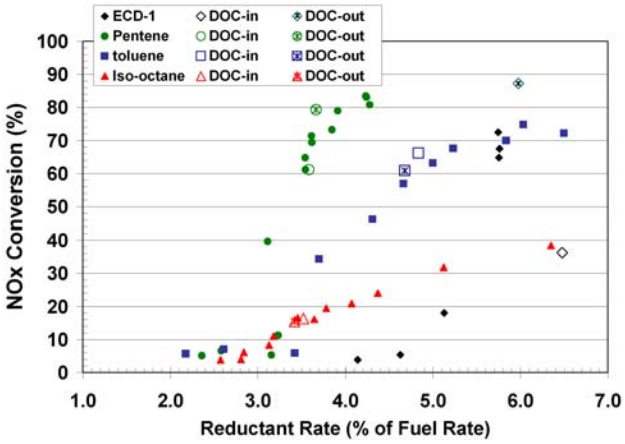

Figure 2. NOx Conversion Versus Reductant Mass Rate

Table 1. Selected Reductant Properties

Compound	Formula	Net Heating Value	Molecular weight	Chemical reduction potential		Stoichiometric mass reductant per g O_2	
		Btu/lb		g O_2/g	Relative to ECD-1	g reductant /g O_2	Relative to ECD-1
toluene	C_7H_8	17,424	92.1	1.56	0.92	0.640	1.08
ECD-1	$CH_{1.87}$	18,480	13.9	1.69	1.00	0.593	1.00
1-pentene	C_5H_{10}	19,255	70.1	1.71	1.01	0.584	0.99
iso-octane	C_8H_{18}	19,080	114.2	1.75	1.04	0.571	0.97

required to consume the same mass of oxygen than a given mass of diesel fuel.

The majority of the results in Figure 2 are for a fixed DOC-inlet injection with a sweep of the DOC-out injection rate (solid symbols), although a few data points are for all reductant injected at the DOC-in (open symbols) or DOC-out (open symbols with *) locations. As expected, as more reductant is delivered, the NOx conversion (y-axis) improves with increasing fuel penalty (x-axis). For the split injection experiments, the injection rate for the DOC-inlet injection was chosen to minimize exhaust oxygen at the NOx adsorber inlet with minimal reductant availability. To set the DOC-inlet injection rate, a careful rate sweep was conducted with no DOC-outlet injection, targeting oxygen contents below 2% with HC peaks below 500 ppm at the NOx adsorber inlet. Although the injection system controls injector duty cycle (on time), effectively controlling reductant *volume*, reductant delivery rates were determined gravimetrically. The split-injection data for ECD-1 are shown as the solid diamonds, while the open diamond and the diamond with * indicate the DOC-in and DOC-out case, respectively. It is interesting that for ECD-1, the system is quite sensitive to the injection location. For the pentene, there may be a similar sensitivity, with the DOC-out injection perhaps better. The toluene and iso-octane show almost no effect of injection location.

With all engine and dynamometer control parameters being the same, the reductant chemistry and reductant mass rate were the only parameters purposely slewed in these experiments. Figure 3 shows the reductant-specific NOx reduction (grams NOx reduced per gram of reductant delivered) versus the reductant mass rate (as a fraction of engine fuel rate). These results further confirm the NOx adsorber catalyst's apparent preference for light alkenes over other HC species. The most efficient HC utilization is apparent for pentene, while performance using iso-octane is very poor. Another valuable metric for reductant utilization is HC emissions. Figure 4 shows the HC emissions (grams HC emitted per gram reductant delivered) versus NOx conversion. This chart shows that over 60% of the iso-octane delivered at the highest reductant delivery rate results in HC emissions. Conversely, the pentene produces the highest NOx reduction with the lowest HC emissions. The ECD-1 outlier point in the upper right is for the DOC-out injection case. Recall from Figure 2 that this case resulted in the highest NOx conversion rates for ECD-1. Unfortunately, the HC emissions for this case are quite high. Conversely, the DOC-out pentene case has high NOx conversion and low HC emissions.

The differences in reductant reactivity led to large differences in the NOx adsorber temperature. Figures 5-8 show the NOx adsorber core temperature for ECD-1, pentene, toluene, and iso-octane reductants, respectively. Each temperature plot has 3 curves, one for each of 3 reductant injection strategies: 1) DOC-in, 2) DOC-out, and 3) split injection. The nomenclature in the legend indicates the injector duty cycle (proportional to spray rate) at

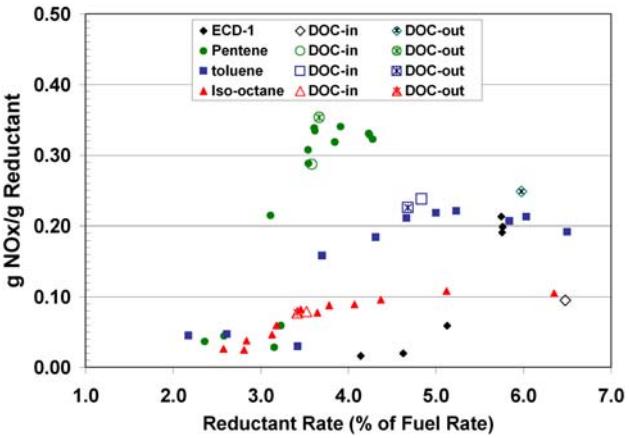

Figure 3. Reductant-Specific NOx Conversion Versus Reductant Mass Rate

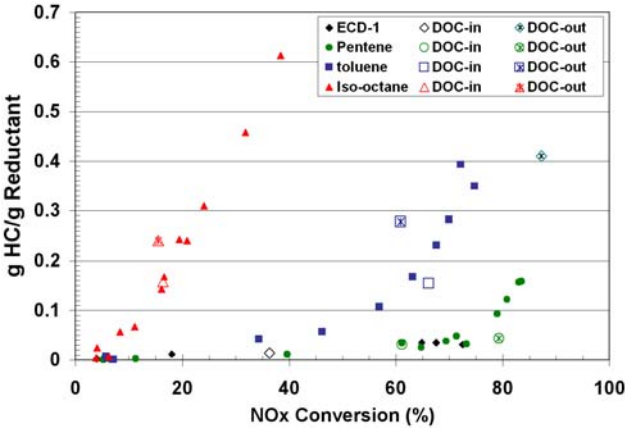

Figure 4. Reductant-Specific HC Emissions Versus Reductant Mass Rate

the two injection points, with the first number indicating the DOC-in duty cycle and the second number indicating the DOC-out duty cycle (e.g., 0.45/0.0 denotes 45% duty cycle on DOC-in injector with zero DOC-out spray). Note the large swings in NOx adsorber temperature in Figure 5 for the ECD-1 case with DOC-out injection. These results are similar to what was reported last year when the DOC was removed. Results for pentene (Figure 6) are similar, and to a lesser extent for toluene (Figure 7). Particularly remarkable are the iso-octane results in Figure 8. Only a small exotherm is notable for the DOC-out injection case.

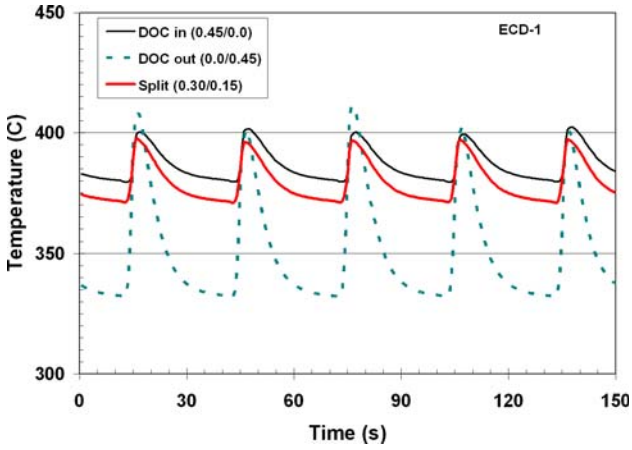

Figure 5. NOx Adsorber Core Temperature for ECD-1 DOC-In, DOC-Out, and Split Reductant Delivery

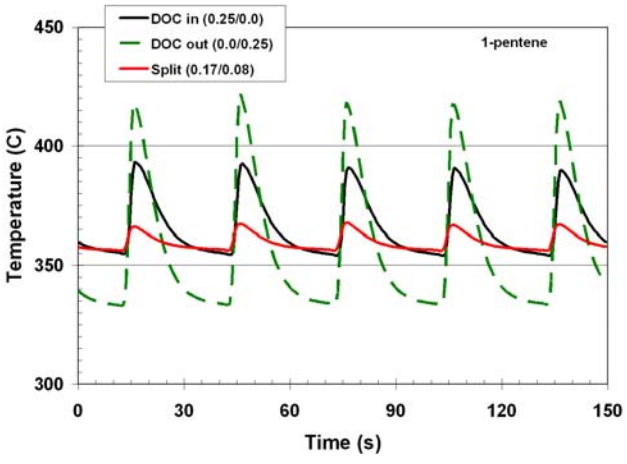

Figure 6. NOx Adsorber Core Temperature for Pentene DOC-In, DOC-Out, and Split Reductant Delivery

Speciation of some light HC compounds was conducted by FTIR, including sampling within the NOx adsorber catalyst bed. These data are still being reduced and will be reported at a later time.

Conclusions

Experiments on NOx adsorber regeneration have been conducted with diesel fuel and 3 pure compounds to examine the HC sensitivity of the catalyst system. Notable conclusions are the following:

- Previously reported findings that light alkenes and monoaromatics appear to be preferred by the

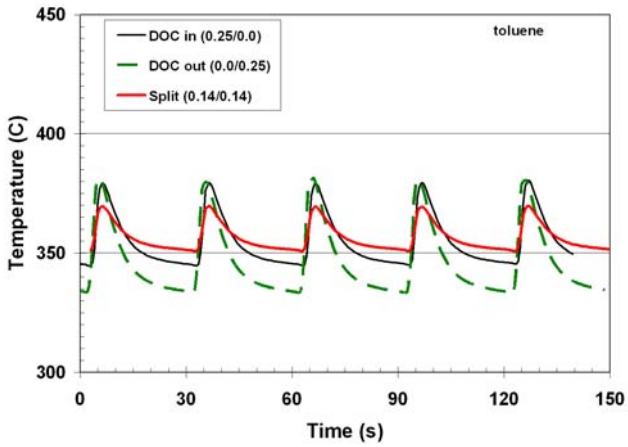

Figure 7. NOx Adsorber Core Temperature for Toluene DOC-In, DOC-Out, and Split Reductant Delivery

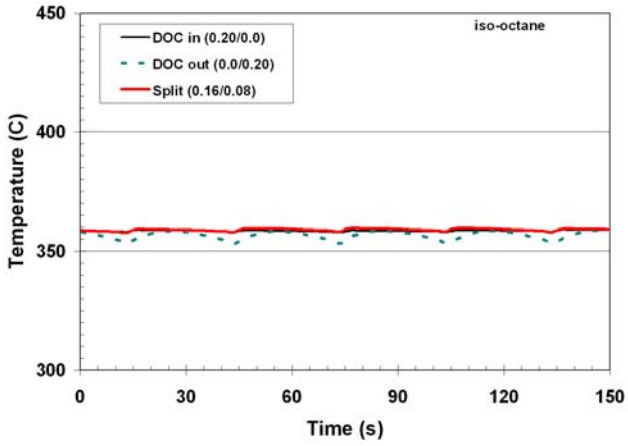

Figure 8. NOx Adsorber Core Temperature for Iso-Octane DOC-In, DOC-Out, and Split Reductant Delivery

NOx adsorber have been confirmed via experiments with pure compounds. For experiments at ~350-400°C:

  - Pentene is the most efficient compound examined, followed by toluene.
  - Iso-octane is very poorly utilized by the NOx adsorber.
  - ECD-1 diesel fuel (largely alkanes) is very effective when oxygen depletion occurs in the NOx adsorber. HC emissions can be problematic.

- Split injection experiments allowed study of oxygen depletion during regeneration in advance of the NOx adsorber or within the NOx adsorber. For experiments at ~350-400°C:
  - Toluene and iso-octane NOx and HC results are less affected by reductant delivery location than ECD-1 or pentene.
  - Best NOx conversion with ECD-1 is found with DOC-out injection, albeit with high HC emissions. It is not clear whether improved NOx conversion for this approach is due to 1) higher temperature during regeneration, with cooler temperatures during NOx loading; 2) an apparent preference for uncracked alkanes; or 3) some combination of 1) and 2).

II.B.6 Advanced CIDI Emission Control System Development

Christine Lambert
Ford Research & Advanced Engineering
P.O. Box 2053, MD 3179
Dearborn, MI 48121

DOE Technology Development Manager: Ken Howden

Subcontractors:
FEV Engine Technology, Inc., Auburn Hills, MI
ExxonMobil Research and Engineering Company (EMRE), Paulsboro, NJ

Objectives

- Develop and demonstrate a highly efficient exhaust emission control system for light-duty compression ignition direct injection (CIDI) engines to meet Federal Test Procedure (FTP) Tier 2 emissions standards of 0.07 g/mi NOx and 0.01 g/mi particulate matter (PM) with minimal fuel economy penalty and 120K mi durability.

Approach

- Conduct parallel engine dynamometer and vehicle testing.
- Continue research to identify the most durable catalysts, filters and exhaust gas sensors.
- Use ultra-low sulfur diesel fuel (15 ppm S, max) to represent U.S. fuel of 2007 and beyond.

Accomplishments

- Tier 2 Bin 5 emissions levels were achieved at low mileage using a selective catalytic reduction (SCR) system with a mid-size diesel engine on a 6,000 lb gross vehicle weight rating (GVWR) light-duty truck. Tailpipe emissions levels were at 0.041 g/mi NOx and 0.001 g/mi PM.
- Durability testing of the emission control system was conducted on an engine dynamometer for 120K mi using the Ford High Speed Cycle, a corporate standard aging cycle.

Future Directions

- Complete evaluation of the 120K mi aged emission control system.
- Continue development of improved catalyst formulations, NOx sensors, and ammonia sensors.

Introduction

Reducing PM and NOx emissions is a primary concern for diesel vehicles required to meet 2007 Federal Tier 2 and California LEVII emissions standards (Table 1). These standards represent a 90-95% reduction from current Federal Tier 1 diesel standards.

The high oxygen content of diesel exhaust makes onboard NOx control complicated. The technology with the most potential to achieve 90+% NOx

Table 1. 2007 FTP Emissions Standards* (passenger cars and light-duty vehicles)

	50K MI		120K MI	
Standard (g/mi)	**NOx**	**PM**	**NOx**	**PM**
LEVII	0.05	----	0.07	0.01
Tier 2, Bin 5	0.05	----	0.07	0.01

*SFTP standards not included.

conversion with minimal or no fuel economy penalty is SCR with an ammonia-based reductant such as aqueous urea. Ammonia-SCR has been used extensively for stationary source NOx control [1]. The main reactions are shown below:

Compared to ammonia, aqueous urea is much safer for onboard vehicle use. Feasibility has been proven by past work at Ford [2,3], Volkswagen [4], Mack Truck [5] and DaimlerChrysler [6].

Control of diesel PM is accomplished with a periodically regenerated ceramic filter, usually called a catalyzed diesel particulate filter (CDPF). The filter may be washcoated with precious metal to help oxidize hydrocarbons (HCs) and collected soot. A diesel oxidation catalyst (DOC) may also be placed upstream of the filter to further aid in filter regeneration. The DOC also provides reduction in HCs and carbon monoxide (CO) emissions, as well as NO oxidation for more durable SCR function.

Approach

At Ford, improved supplier catalysts were tested in laboratory flow reactors for aged conversion levels. The best performing system that included a DOC, SCR catalyst, and CDPF was aged and tested on an engine dynamometer at FEV. Ultra-low sulfur diesel fuel (<15 ppm S) was used for all aging and testing. Interim tests of the aged system were performed on a 6,000 lb GVWR light-duty truck (LDT). Appropriate exhaust gas sensors and control strategies were tested for durable system function. System modeling played an important role in design. Hardware for delivery of aqueous urea to light-duty diesel vehicles was completed.

Results

Over 90% NOx conversion was achieved at low mileage with a system of DOC, urea SCR, and CDPF on a 6,000 lb LDT. The average tailpipe emissions on the FTP-75 test were 0.042 g/mi non-methane organic gases (NMOG), 2.0 g/mi CO, 0.047 g/mi NOx, and 0.002 g/mi PM, all below Tier 2 Bin 5 standards. Engine-out NOx was reduced approximately 40% through the use of higher levels of exhaust gas recirculation (EGR). A rapid warm-up procedure was used during the cold-start portion of the test cycle.

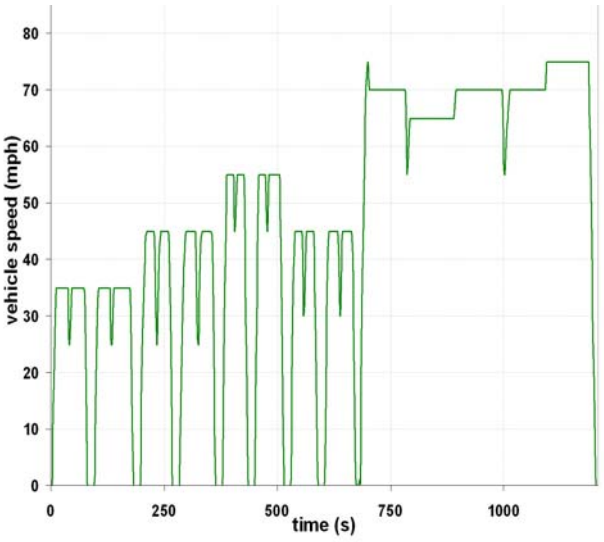

Figure 1. Vehicle Speed Trace for the Ford High Speed Cycle

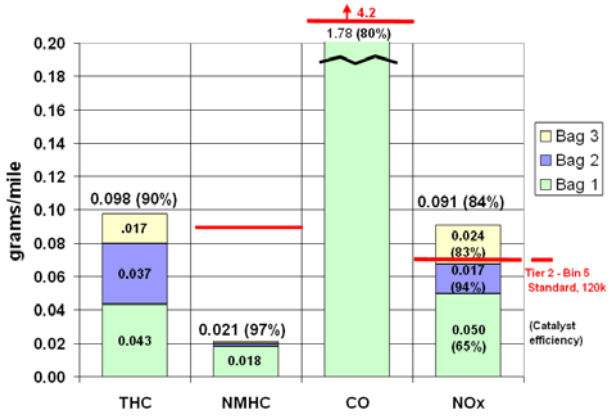

Figure 2. FTP-75 Performance of the 50K mi Aged Catalyst System on the 6,000 lb GVWR LDT Without Rapid System Warm-Up

After successfully testing the urea SCR and CDPF system in the fresh state, the system was aged on the engine dynamometer for 50K mi using the Ford High Speed Cycle, the corporate standard aging cycle. The vehicle speeds used for this cycle are shown in Figure 1. The cycle was repeated on the engine dynamometer at FEV for 24 h per day, five to six days per week. The DOC was used to generate the required exotherm for soot oxidation, regularly raising the SCR catalyst and CDPF to temperatures in excess of 650°C.

At the 50K mi mark, the system performance was tested on the FTP-75 with the LDT, as shown in Figure 2. Difficulty occurred during implementation

of rapid warm-up during cold-start due to the prototype nature of the engine. It was apparent that the Tier 2 Bin 5 50K mi NOx standard (0.05 g/mi) was exceeded due to low NOx conversion during cold-start (Bag 1). However, the average FTP-75 tailpipe NOx at 50K mi was similar to performance at low mileage without rapid warm-up (0.13 g/mi NOx), indicating that the SCR catalyst had not significantly aged.

A prediction of NOx emissions at 50K mi if rapid warm-up had been available was performed. The inlet temperature to the SCR catalyst during the first phase (0 - 505 s) of the FTP-75 was much lower without rapid warm-up. This resulted in a higher level of tailpipe NOx (0.076 g/mi) in that particular 50K mi test. An earlier test at low mileage with warm-up resulted in less than 0.05 g/mi NOx. It was predicted that if the 50K mi test had behaved similarly to the low mileage test in the first 200 s of the test cycle, the tailpipe NOx would have been approximately 0.05 g/mi NOx, meeting the Tier 2 Bin 5 standard.

New urea SCR catalysts were aged and tested in the laboratory flow reactor to widen the temperature window for durable, high NOx conversion. A catalyst with greatly improved low-temperature performance was recently received, as well as two with improved high-temperature performance.

Both NOx and NH_3 sensors were studied in the laboratory and onboard the project vehicle. A pre-production NOx sensor was used upstream of the underbody oxidation catalyst to ensure that the correct amount of urea solution was injected during transient operation. An ammonia sensor was successfully tested on the F250 project vehicle when located between the SCR catalyst and the CDPF.

Conclusions

- The objective of 0.07 g/mi NOx and 0.01 g/mi PM on the FTP was met with a fresh emission control system of urea SCR and CDPF on a light-duty truck. HC, CO and PM emissions at 50K mi met Tier 2 Bin 5 standards.
- NOx emissions at 50K mi were 0.09 g/mi and were predicted to be 0.05 g/mi (Bin 5) if rapid warm-up during cold-start was functional.
- New SCR catalysts were developed that have improved NOx conversion after 120K mi equivalent aging.
- Prototype NH_3 sensors were successfully tested on a vehicle.

FY 2005 Publications/Presentations

1. C. Lambert, et al., "Urea SCR and DPF System for Diesel Sport Utility Vehicle Meeting Tier 2 Bin 5," 2005 DEER Conference.

References

1. R.M. Heck and R.J. Farrauto, *Catalytic Air Pollution Control*, Van Nostrand Reinhold, NY, 1995.
2. H. Luders, R. Backes, G. Huthwohl, D.A. Ketcher, R.W. Horrocks, R.G. Hurley, and R.H. Hammerle, "An Urea Lean NOx Catalyst System for Light Duty Diesel Vehicles," SAE 952493.
3. P. Tennison, C. Lambert and M. Levin, "NOx Control Development with Urea SCR on a Diesel Passenger Car," SAE 2004-01-1291.
4. W. Held, A. Konig, T. Richter, L. Puppe, "Catalytic NOx Reduction in Net Oxidizing Exhaust Gas," SAE 900496.
5. W.R. Miller, J.T. Klein, R. Mueller, W. Doelling, J. Zuerbig, "The Development of Urea-SCR Technology for US Heavy Duty Trucks," SAE 2000-01-0190.
6. W. Mueller, H. Ölschlegel, A. Schäfer, N. Hakim and K. Binder, "Selective Catalytic Reduction - Europe's NOx Reduction Technology," SAE 2003-01-2304.

II.B.7 Development of Improved SCR Catalysts

Eric N. Coker
Sandia National Laboratories (SNL)
Ceramic Processing and Inorganic Materials
P.O. Box 5800, MS 1349
Albuquerque, NM 87185-1349

Cooperative Research and Development Agreement (CRADA) Partners: Low Emissions Technologies Research and Development Partnership
(Member Companies: DaimlerChrysler Corporation, Ford Motor Company, and General Motors Corporation)

DOE Technology Development Manager: Ken Howden

Technical Advisors:
John Hoard (Ford Motor Company)
Christine Lambert (Ford Motor Company)
Richard Blint (General Motors)

Objectives

- Develop new catalyst technology to enable compression ignition direct injection (CIDI) engines to meet Environmental Protection Agency (EPA) Tier II emissions standards with minimal impact on fuel economy.
- Optimize catalyst formulations for activity, stability, and resistance to poisoning.
- Demonstrate feasibility for scale-up of preparation of promising catalysts.
- Transfer technology of most promising formulations to catalyst suppliers via original equipment manufacturers (OEMs).

Approach

- Design and develop new non-vanadia, hydrous metal oxide (HMO)-based catalyst materials for reducing NOx emissions in lean-burn exhaust environments using ammonia as a reductant.
- Test catalyst formulations under realistic laboratory conditions using a protocol developed with Low Emissions Partnership (LEP) input.
- Where appropriate, transfer successful powder catalyst formulations to monolith platform and re-evaluate.
- Evaluate short-term durability under hydrothermal conditions and in the presence of SO_2/SO_3.
- Characterize catalysts using a variety of techniques to gain understanding of critical parameters related to activity and aging phenomena.
- Scale up synthesis and processing of promising catalyst formulations to enable fabrication of prototype catalytic converters for CIDI engine dynamometer testing.
- Enable technology transfer of the most promising catalyst formulations and processes to designated catalyst suppliers *via* the LEP.

Accomplishments

- Several new catalyst formulations showed enhanced NOx conversion performance compared to the commercial ZNX catalyst material.

Future Directions

- This CRADA project has ended.

Introduction

This report covers the end of a multi-partner effort which involved separate CRADAs between three national laboratories (Los Alamos National Laboratory [LANL], Oak Ridge National Laboratory [ORNL], and Sandia National Laboratories [SNL]) and the Low Emissions Technologies Research and Development Partnership (LEP, composed of DaimlerChrysler Corporation, Ford Motor Company, and General Motors Corporation). The CRADAs with LANL and ORNL ended in FY 2004 (the FY 2004 Annual Report was their final contribution), and the SNL CRADA ended April 29th, 2005.

The project addressed reduction of CIDI engine NOx emissions using exhaust aftertreatment – identified as one of the key enabling technologies for CIDI engine success. The overall CRADA efforts were focused on the development of urea/ammonia selective catalytic reduction (SCR) processes for reducing NOx emissions, specifically targeting the selection of appropriate catalyst materials to meet the exhaust aftertreatment needs of light- and medium-duty diesel engines (SNL and LANL) and understanding of the urea-catalyst interaction as well as factors influencing urea decomposition (ORNL). Infrastructure issues notwithstanding, the SCR process has the greatest potential to successfully attain the >90% NOx reduction required for CIDI engines to meet the new EPA Tier II emissions standards phased in starting in 2004.

Approach

SNL continued to develop catalysts supported on hydrous metal oxides (HMOs). New catalyst formulations were investigated, with emphasis on enhancing low-temperature activity. During FY 2005 we focused on testing catalysts under more stringent testing conditions, with particular attention paid to benchmarking of SNL catalysts against a commercial material (ZNX, from Engelhard).

Standard experimental details for catalyst evaluation are summarized in Table 1 together with performance targets under each set of conditions.

Table 1. Standard Conditions Used in Bench Reactor Evaluation of SCR Catalyst Performance, and Performance Targets Developed in Conjunction with the LEP

	Standard Test Conditions I ($NO:NO_2$ = 1:1)	**Standard Test Conditions II ($NO:NO_2$ = 4:1)**
Temperature	450 - 125°C	450 - 125°C
GHSV (h^{-1}) [monolith]	30,000	30,000
GHSV (h^{-1}) [powder]*	120,000 - 140,000	120,000 - 140,000
NO (ppm)	175	280
NO_2 (ppm)	175	70
NH_3 (ppm)	350	350
O_2 (%)	14	14
CO_2 (%)	5	5
H_2O (%)	4.6	4.6
Balance	N_2	N_2
NOx conversion target, 200°C (%)	90	50
NOx conversion target, 200 – 400°C (%)	90	N/A

*Powders tested at standard flow rate of 3.125 Liters (g catalyst)$^{-1}$ min^{-1}; GHSV varies depending on catalyst density.

Results

Following some extended down-time of the SNL bench test reactor and extensive troubleshooting and re-calibration of equipment as reported in the FY 2004 annual report, considerable time was spent evaluating a benchmark catalyst (ZNX monolith core, from Engelhard) on the SNL system in order to establish limits of reproducibility and reliability. Good reproducibility of data was obtained, as shown in Figure 1 for several successive runs using the same monolith core. Note that a small deactivation was noticed after the first run, but NOx conversion

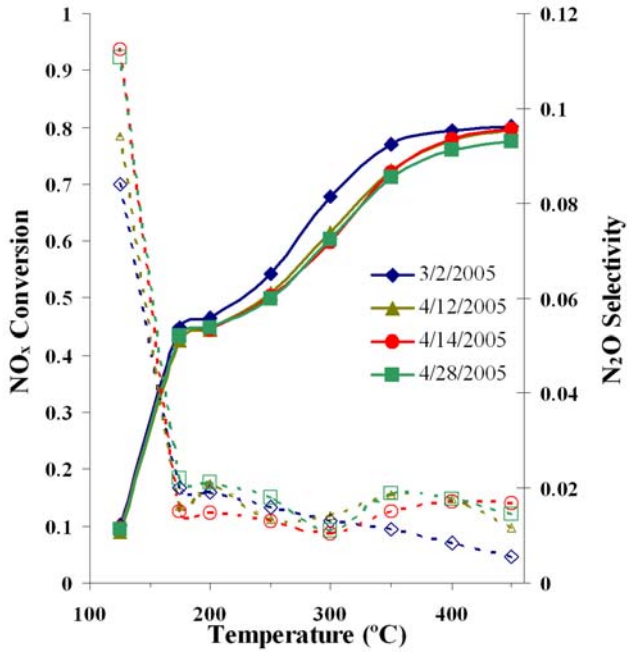

Figure 1. Performance of a ZNX monolith core evaluated in four tests over a two-month period after the SNL bench test reactor was re-commissioned. Experimental conditions as in Table 1, with $NO:NO_2 = 4:1$. Solid line = NOx conversion; dashed line = N_2O selectivity.

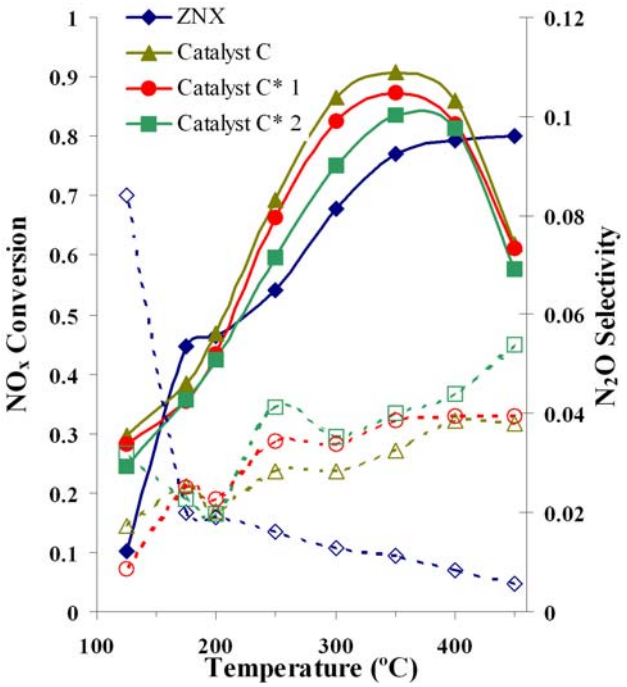

Figure 2. Performance of a ZNX monolith core and three powder catalysts developed at SNL: Catalyst C, Catalyst C*1 and Catalyst C*2. Experimental conditions as in Table 1, with $NO:NO_2 = 4:1$. Solid line = NOx conversion; dashed line = N_2O selectivity.

profiles and N_2O selectivity were constant thereafter. Similar results were obtained for different monolith cores of ZNX and are not shown. Since the intrinsic performance of a standard catalyst will often vary depending upon the apparatus on which it is evaluated, all data in this report is compared with ZNX measured under equivalent conditions and on the same apparatus. Indeed, the intrinsic ZNX performance measured on the SNL bench test apparatus is typically lower than that measured under comparable conditions on other bench test reactors. The reason for this difference in baseline performance is not known. All NOx conversion data are compared to ZNX in this report, with the assumption that the relative performances of a new catalyst and ZNX will be similar on a different bench test reactor.

A range of catalyst formulations, based on a previous high-performing catalyst (Catalyst C in previous reports), was prepared and tested under the conditions given in Table 1; these catalysts are designated "Catalyst C*n", where n is an integer. Catalyst C had shown performance satisfying all of the selection criteria for a viable urea-SCR catalyst, viz: NOx conversion activity and selectivity in the fresh, hydrothermally aged, and sulfur-treated forms. Catalysts C* are differentiated from Catalyst C in that they possess metal-oxide components in addition to those of Catalyst C. That is to say, each new catalyst was prepared by adding one or more metal oxides to a common starting material of Catalyst C. Furthermore, the performance of each new catalyst was compared against the commercial benchmark catalyst ZNX (the first data set from Figure 1, i.e., that showing the highest activity for ZNX). The ZNX was tested in monolith core form, while the SNL-developed catalysts were evaluated as powders using the appropriate gas flow conditions given in Table 1. Prior work has shown that comparison of monolith core and powder data is valid provided the gas flow rates for the powder are adjusted to simulate those seen by the catalyst in a monolithic catalyst [1].

Figure 2 compares the NOx conversion performance and N_2O selectivity for ZNX, Catalyst

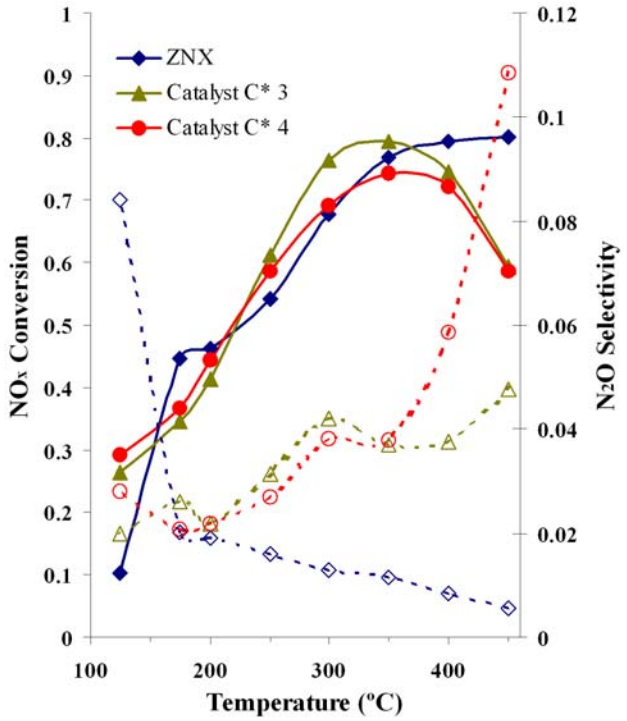

Figure 3. Performance of a ZNX monolith core and two powder catalysts developed at SNL: Catalyst C*3 and Catalyst C*4. Experimental conditions as in Table 1, with NO:NO_2 = 4:1. Solid line = NOx conversion; dashed line = N_2O selectivity.

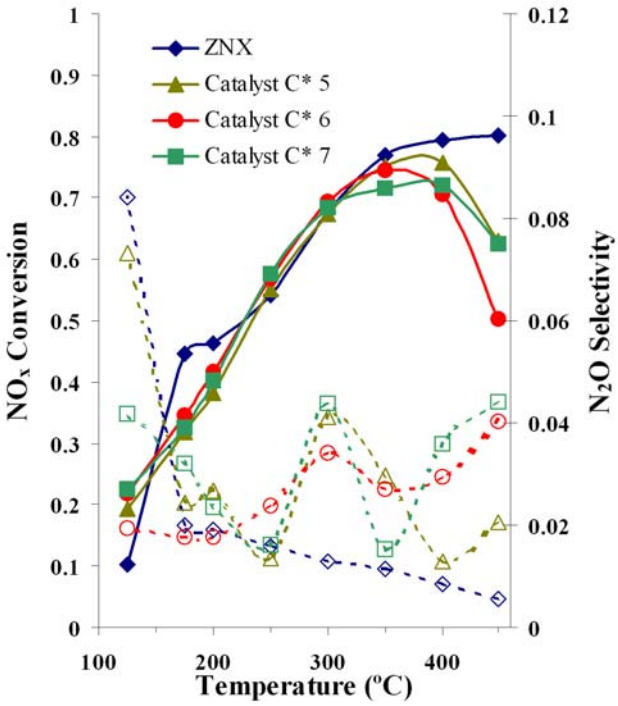

Figure 4. Performance of a ZNX monolith core and three powder catalysts developed at SNL: Catalyst C*5, Catalyst C*6 and Catalyst C*7. Experimental conditions as in Table 1, with NO:NO_2 = 4:1. Solid line = NOx conversion; dashed line = N_2O selectivity.

C, Catalyst C*1 and Catalyst C*2. It is noteworthy that Catalyst C outperforms ZNX over almost the entire temperature window studied. Each of the C* catalysts in this figure also offer enhanced NOx conversion relative to ZNX over the majority of the temperature window, but are not as active as Catalyst C.

Two other C* catalysts performed as well as or better than ZNX over the middle temperature range (250 – 350°C, Catalysts C*3 and C*4, Figure 3), while the remainder were generally less active than ZNX (Catalysts C*5, C*6 and C*7, Figure 4).

Thus, the C* catalysts offered no advantage over Catalyst C in the fresh (un-aged) state; however, given the enhanced performance of a few of the new catalysts compared to ZNX, investigation of their hydrothermal durability and sulfur tolerance may reveal advantages over previous catalyst formulations.

Conclusions

- Benchmarking with a ZNX monolith core verified stable operation of the SNL bench test reactor system after extended maintenance and troubleshooting.
- New catalyst formulations based on previously-reported Catalyst C were prepared and evaluated.
- Two new formulations out-perform ZNX over the majority of the temperature window.
- Two additional new formulations out-perform ZNX over the middle-temperature range (250 – 350°C).
- Catalyst C offers better NOx conversion performance than new formulations in the fresh (un-aged) state.

FY 2005 Publications/Presentations

1. "Development of durable low-temperature urea-SCR catalysts for light-duty mobile CIDI engines," D.A. Peña, J.N. Stuecker, E.N. Coker, J. Cesarano III, J.E. Miller, *29th International Cocoa Beach Conference and Exposition on Advanced Ceramics & Composites*, Cocoa Beach, FL, January 23-28, 2005.

References

1 E.N. Coker, J.M. Storey and K.C. Ott, "Development of improved SCR catalysts," *Advanced Combustion Engine Research and Development, 2004 Progress Report*, DOE-OFCVT, pp.166-179.

II.B.8 Quantitative Identification of Surface Species on Lean NOx Traps, DOE Pre-Competitive Catalyst Research

Todd J. Toops (Primary Contact), D. Barton Smith, W. William Partridge, Jim E. Parks
Oak Ridge National Laboratory (ORNL)
2360 Cherahala Blvd.
Knoxville, TN 37932

DOE Technology Development Manager: Ken Howden

Objectives

- Provide a better understanding of the fundamental deactivation mechanisms that result during regeneration and desulfation of lean NOx traps (LNTs)
- Transfer this information to:
  - improve the material
  - improve the desulfation methods
  - improve simulation of the processes

Approach

- Effort is pre-competitive
- Compare "fully-formulated" catalysts in coordination with manufacturers
- Study deactivation mechanism fundamentally
- Evaluate thermal aging independent of sulfur
- Evaluate deactivation from sulfur poisoning and desulfation
- Employ multiple analytical techniques to monitor activity and morphology effects
- Disseminate results and data

Accomplishments

- Modified reactors to allow key LNT measurements
- Demonstrated fully-formulated catalyst deactivation similar to model catalysts
- Characterized effects of thermal aging on model catalysts at the surface level
- Mapped desulfation for model catalysts
- Analyzed sulfation and desulfation at surface
- Developed new reactor for Diffuse Reflectance Infrared Fourier-Transform Spectroscopy (DRIFTS) measurements along length of washcoat

Future Directions

- Continue activity characterization for thermal and sulfur tests
- Quantify DRIFTS spectra for K-based catalyst
- Expand temperature range (200 and 500°C)
- Further characterize catalysts with respect to sulfation
- Implement *in-situ* DRIFTS reactor for washcoated samples

Introduction

Several efforts previously investigated under the Cummins/ORNL Cooperative Research and Development Agreement (CRADA) which are pre-competitive have been transferred to this project. This allows open dissemination of those research results, without confusing issues of CRADA-protected information, and frees up CRADA funds to investigate protected topics. The transferred efforts connect kinetic rates with optical spectroscopy areas. Nevertheless, the two projects will continue to work closely to address both competitive and pre-competitive research issues.

The complex heterogeneous nature of production catalyst washcoats critically obscures research of fundamental mechanisms. Model catalyst materials represent only a component of production materials, but allow isolation of individual fundamental processes; these include detailed mechanisms for desorption and poisoning, intermediate existence and roles, and reduction details. Hence, this project primarily employs model catalyst materials for experimental investigation of fundamental catalyst phenomena.

Approach

Under future vehicle regulations, the efficiency of a diesel engine system will be correlated to the efficiency of the catalyst system since a fuel penalty is sustained to achieve the emissions requirements. Therefore, it is essential to have an efficiently functioning catalyst system in operation with a diesel engine. Modeling/simulating processes is an effective way to develop efficient systems, and basing the model on fundamental chemistry is critical for it to be transportable and broadly useful to industry; parametric-based models will not fill the need.

The emphasis of this project is to improve detailed understanding of mechanisms limiting catalyst performance. The work will be conducted in conjunction with catalyst industry representatives to identify and investigate pre-competitive catalyst performance issues of broad relevance across the catalysis industry. Specific objectives are to improve the fundamental understanding of adsorption, reduction, and poisoning processes, and to determine the influence of catalyst morphology. The objectives of this project are consistent with those of the Diesel Cross-Cut Team regarding details of sulfur poisoning and catalyst morphology effects.

Results

The experimental investigations during the past year led to several key findings that relate fundamental sulfur and thermal deactivation observation with events observed on the engine. Furthermore, these findings suggest key considerations for both modeling endeavors and engine strategies. Two model LNTs, $Pt/K/Al_2O_3$ and $Pt/Ba/Al_2O_3$, were studied extensively, and a "fully-formulated" LNT obtained from Delphi was also investigated to verify the trends of the model catalysts. The catalysts were first thermally aged without sulfur to isolate the temperature effects associated with heating the catalysts up to 900°C, and then a separate sulfation/desulfation protocol was followed.

Thermal deactivation tests at 760 and 900°C were run on Delphi's Ba-based LNT catalyst, and the results compared very favorably with the model catalysts, as shown in Figure 1. As with the model catalysts, the Delphi sample was generally able to maintain its surface area (Figure 1a), but it showed a significant decrease in total NOx storage capacity above 760°C (Figure 1c). Due to the complexity of the Delphi catalyst, it was not possible to measure the Pt sintering while aging; the post 900°C dispersion was measured ex-situ with x-ray diffraction (Figure 1b). Since Pt size was unable to be probed in-situ and it is important to have some measure of its impact, the overall NOx conversion was measured under a fast lean/rich cycle (60 s lean/5 s rich) for the Delphi catalyst. This approach will take into account the effects of both Pt size, which is necessary for both storage and reduction, and storage capacity. The overall NOx conversion on the Delphi catalyst was initially 62%, as shown in Figure 1d, but after aging for 10 h at 760°C it dropped to 41%, and then to 20% after aging at 900°C.

Having established a baseline of the independent effects of thermal excursions, it was appropriate to study the deactivation incurred by sulfur and high-

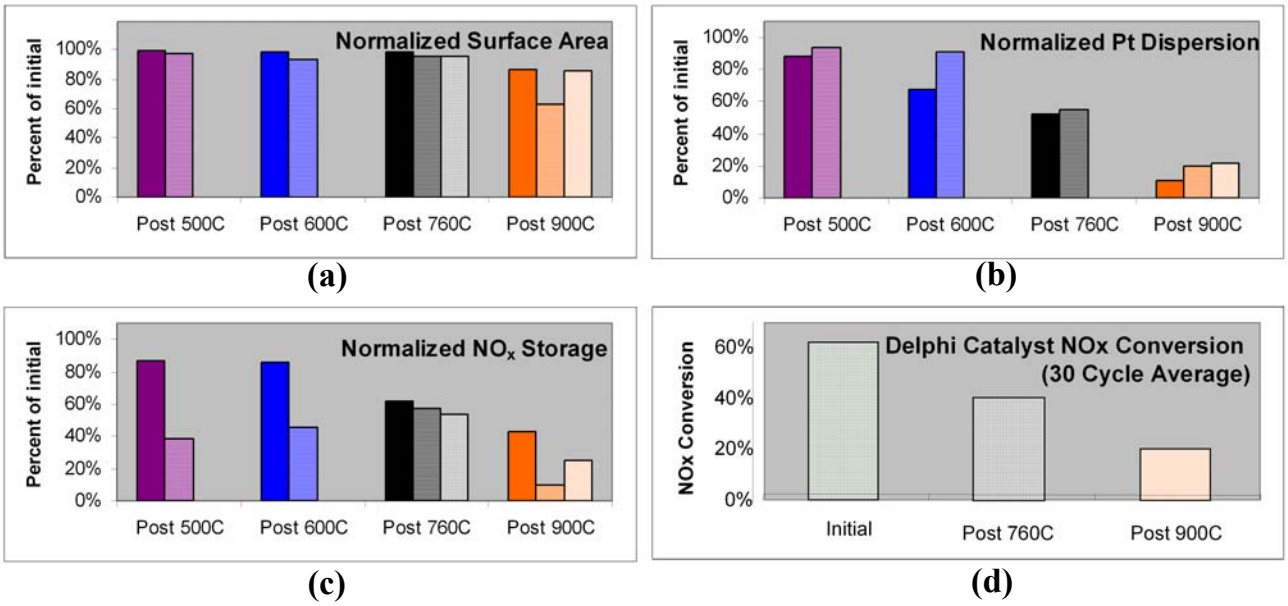

Figure 1. Comparison of the effects of thermal aging after 500°C, 600°C, 760°C, and 900°C with respect to (a) surface area, (b) Pt dispersion, (c) NOx storage at saturation, and (d) NOx Conversion. Data shown in (a)-(c) is displayed with respect to the initial catalyst values, while (d) is actual NOx conversion averaged over 30 lean/rich cycles. Catalysts studied: (■) $Pt/K/Al_2O_3$, (▤) $Pt/Ba/Al_2O_3$, and (▨) Delphi's fully-formulated catalyst.

temperature desulfation. The catalysts were severely poisoned with SO_2 under lean operation at 250°C. Initial desulfation tests up to 760°C using temperature-programmed reaction (TPRX) in H_2 at 20°C/min showed that there were generally two levels of significant desulfation; one occurred just below 500°C and the other near 700-750°C. Based on this knowledge, subsequent tests were carried out in two tiers with activity, surface characterization, and capacity measurements taken after sulfation, desulfation at 500°C, and desulfation at 760°C. These measurements are compared to the initial activity in Figure 2a and show that desulfation of a heavily sulfated catalyst can restore up to 95% of the NOx activity using typical engine LNT lean/rich cycles (based on short cycle NOx conversions with 60 s lean and 5 s rich). This finding is very interesting, especially since saturation measurements show a decrease in storage sites by 55-62%. This illustrates the loss of sites that are associated with long-term adsorption, but also the quick recovery of the critical fast adsorption sites. This effect is further illustrated by the breakthrough curves in Figure 2b for $Pt/K/Al_2O_3$ and Figure 2c for $Pt/Ba/Al_2O_3$.

An oddity was also observed during the desulfation experiments regarding differences in the expected form of sulfur at high temperatures. Mass spectrometry is being used to monitor the effluent during the TPRX experiments, and during the desulfation experiments up to 760°C, a large quantity of H_2 is reacted, with the expected amount of H_2O being formed; however, there is a discrepancy in the amount of observed sulfur products, as displayed in Figure 3a for $Pt/K/Al_2O_3$ and Figure 3b for $Pt/Ba/Al_2O_3$. Essentially, the quantity of measured SO_2 and H_2S is a factor of 2-5 times less than the predicted product quantities based on their reactions with H_2. There is generally good agreement for the low-temperature desulfation, within 10-20%, but this large discrepancy at higher temperatures suggests another reaction is occurring. The unobserved sulfur during desulfation could be residing in the form of Pt sulfide. This can be mitigated by periodically switching to lean conditions during the desulfation; additionally, the presence of H_2O and CO_2 during desulfation may inhibit this sulfide formation. Preliminary experiments have been run to investigate the effects of CO_2 and H_2O during desulfation, and initial results show that there is much less excess H_2

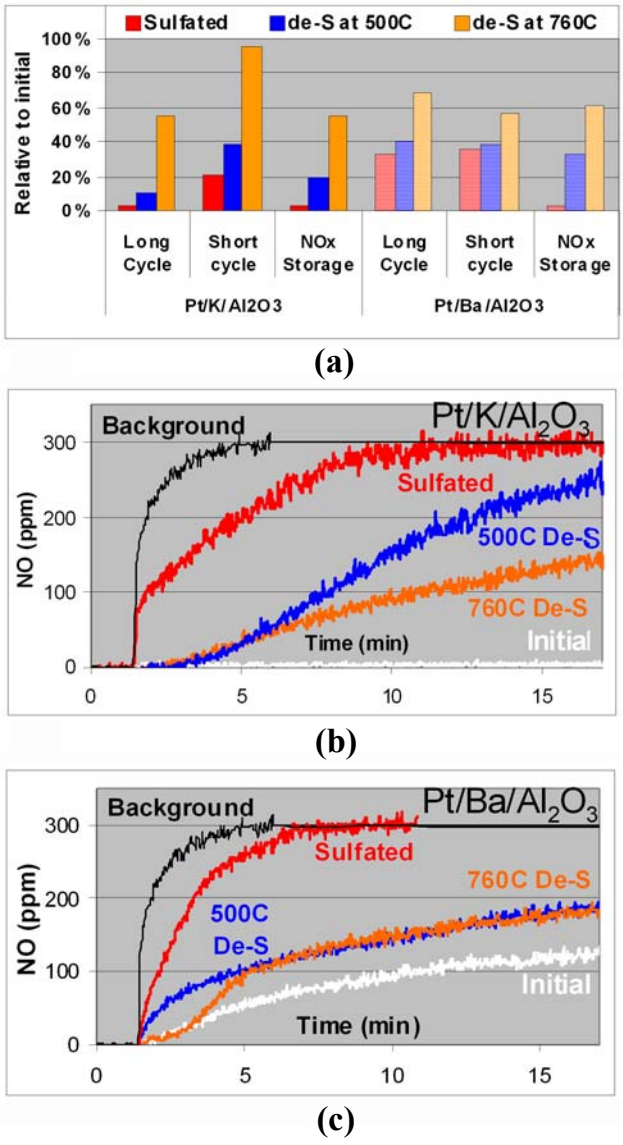

Figure 2. (a) Effects of sulfation and desulfation on activity of model catalysts (long cycle: 15 min lean/10 min rich, short cycle: 60 s lean/5 s rich, NO_x storage at saturation). Breakthrough curves for (b) $Pt/K/Al_2O_3$ and (c) $Pt/Ba/Al_2O_3$ demonstrate the similarity in storage behavior following desulfation at 760°C in the first couple of minutes of lean operation.

reacted, which supports the proposed explanation of Pt-S formation. Future experiments will employ other characterization techniques that will try to track this formation.

To investigate the effects at the catalyst surface, DRIFTS measurements were performed on the model K and Ba catalysts during sulfation and

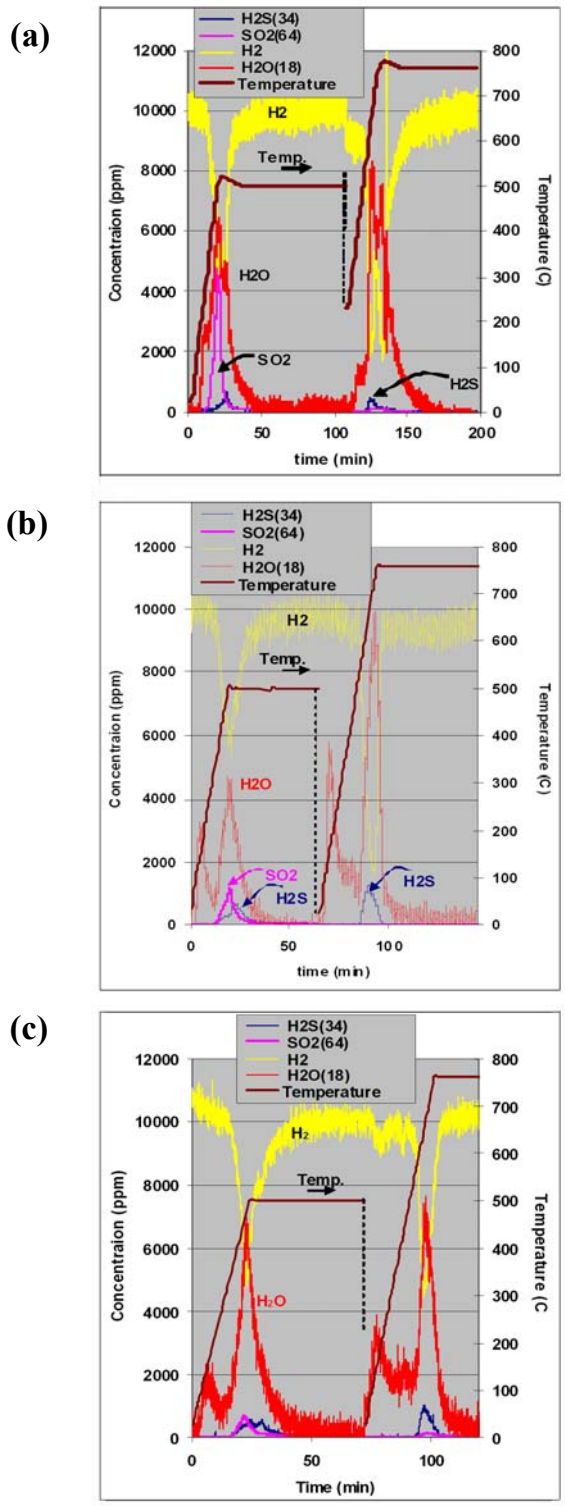

Figure 3. TPRX curves for the two-tiered desulfation of (a) $Pt/K/Al_2O_3$, (b) $Pt/Ba/Al_2O_3$, and (c) Delphi's fully-formulated LNT. The high-temperature desulfation demonstrates a discrepancy between amount of H_2 reacted and the amount of sulfur products formed.

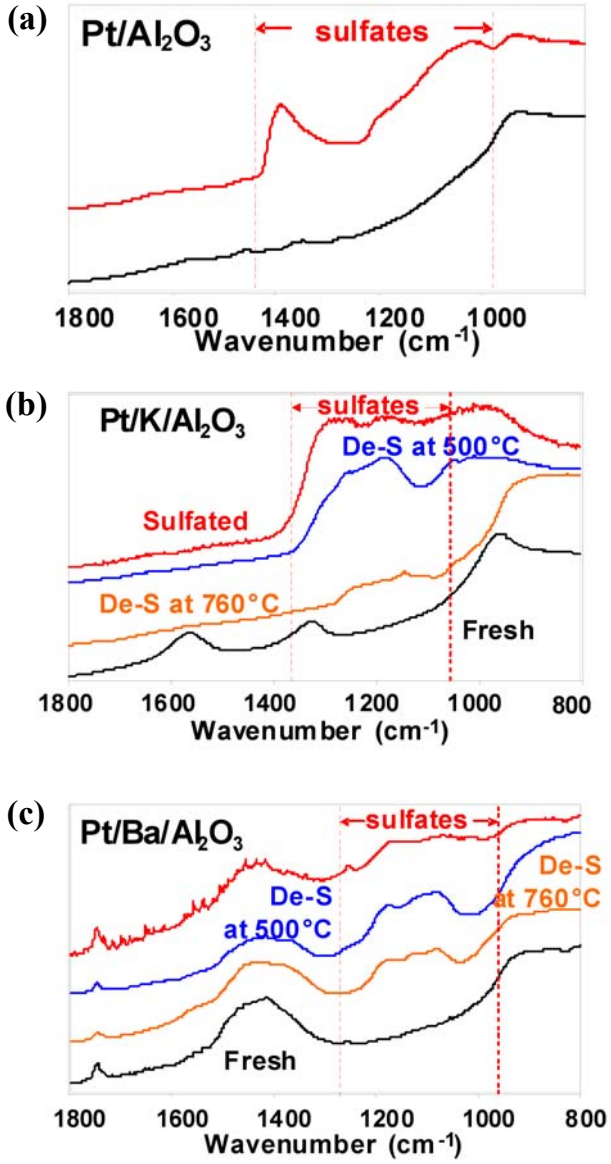

Figure 4. DRIFTS analysis of (a) Pt/Al_2O_3, (b) $Pt/K/Al_2O_3$ and (c) $Pt/Ba/Al_2O_3$ during various stages of ex-situ desulfation. Sulfur still remains on each of the catalysts. Sulfates formed on Pt/Al_2O_3 do not directly coincide with the majority of the sulfates on the LNT catalysts.

following ex-situ desulfation at 500 and 760°C. The key observation in this study, as evidenced in Figure 4, was that even after desulfation at 760°C, significant sulfates still remain on the surface of the catalyst, especially the Ba-based LNT.

The goal of performing the thermal aging tests in the absence of sulfur was to define the primary

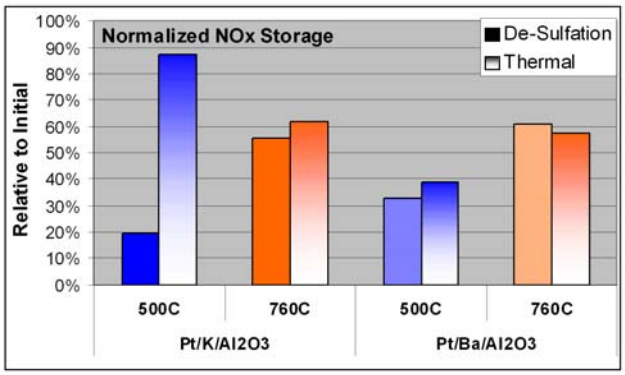

Figure 5. Comparison of NOx storage for model catalysts that have been sulfated and then desulfated at 500 and 760°C to those that have only been thermally aged at 500 and 760°C.

deactivation mechanisms in LNTs at certain temperatures. A direct comparison of storage losses after 500°C and 760°C demonstrated that sulfur poisoning will generally dominate at 500°C and thermal aging will be the prevailing factor above ~700°C. Figure 5 shows that even though the catalysts are not completely sulfur-free after 760°C, the deactivation caused by thermal aging only is on par with the partially poisoned desulfated catalysts.

The model catalyst results compare well with the engine tests and also show that the model catalysts were more heavily poisoned. The most important trend that can be shown in this comparison is that desulfation above 700°C will permanently deactivate the catalyst. Engine strategies should consider low-temperature desulfation for longer periods as a possible solution to LNT deactivation, as short high-temperature bursts could irreversibly deactivate the LNT.

Our design for a DRIFTS reactor will enable *in-operando* investigation of surface species along the length of washcoated sample. Figure 6 shows a detailed cross-section of the reactor and the Barrel Ellipse DRIFTS attachment. The reactor is designed to allow flow between the infrared window and the sample. The catalysts sample can have dimensions that are 25 mm wide and up to 300 mm in length. This reactor is designed to allow surface investigations along the axial length of washcoated samples. When coupled with spatially-resolved capillary inlet mass spectrometry, this instrument

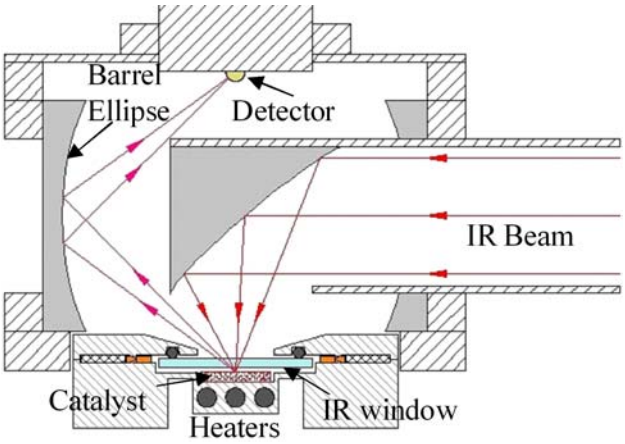

Figure 6. Schematic of monolithic DRIFTS reactor and Barrel Ellipse DRIFTS attachment. Gas will flow between catalyst and the IR window. Washcoated catalysts can be up to 25 mm wide (as shown) and 300 mm long.

will be a powerful tool that will allow a direct correlation between observed surface species and gas-phase concentrations.

Conclusions

- New reactor designs allow a more complete analysis of LNT deactivation.
- Model catalysts are reasonable approximations of fully-formulated catalysts.
- Thermal aging is the primary mechanism of LNT deactivation.
- Desulfation is very slow and most likely does not ever produce a sulfur-free catalyst.
- Desulfating under rich conditions only will result in Pt-S formation.
- Longer desulfation at low temperature may be an option.

FY 2005 Publications/Presentations

1. T.J. Toops, D.B. Smith, W.P. Partridge, "NOx Adsorption on Pt/K/Al_2O_3," accepted to Catalysis Today.
2. T.J. Toops, D.B. Smith, W.P. Partridge, "Quantification of the *in-situ* DRIFT Spectra of Pt/K/gamma-Al_2O_3 NO_x Adsorber Catalysts," Applied Catalysis B: Environmental 58 (2005) 245.
3. T.J. Toops, D.B. Smith, W.S. Epling, J.E .Parks, W.P. Partridge, "Quantified NOx Adsorption on Pt/K/gamma-Al_2O_3 and the Effects of CO_2 and H_2O," Applied Catalysis B: Environmental 58 (2005) 255.
4. T.J. Toops, W.P. Partridge and D.B. Smith, "Fundamental Study of Lean NOx Trap Deactivation," DOE Advanced Combustion Engine Review Meeting, Argonne, IL, USA, 04/19/2005-04/21/2005.
5. T.J. Toops, D.B. Smith and W.P. Partridge, "Lean NOx Trap Aging and Deactivation," CLEERS 8th DOE Crosscut Workshop, Detroit, MI, USA, 05/17/2005-05/19/2005.
6. T.J. Toops, W.P. Partridge and D.B. Smith, "Deactivation of Model Lean NO_x Traps," 19th Meeting of the North American Catalysis Society, Philadelphia, PA, USA, 05/22/2005-05/27/2005.
7. T.J. Toops, W.P. Partridge and D.B. Smith, "Lean NO_x Trap Adsorption on Pt/K/Al_2O_3," 19th Meeting of the North American Catalysis Society, Philadelphia, PA, USA, 05/22/2005-05/27/2005.

II.B.9 NOx Control and Measurement Technology for Heavy-Duty Diesel Engines

Bill Partridge (Primary Contact), Jae-Soon Choi, Norberto Domingo
Oak Ridge National Laboratory
2360 Cherahala Blvd.
Knoxville, TN 37932

DOE Technology Development Manager: Ken Howden

Cooperative Research and Development Agreement (CRADA) Partner:
Cummins Inc., Tom Yonushonis, Neal Currier, Bill Epling, John Stang, Mike Ruth

Objectives

- Improve diesel engine-catalyst system efficiency through detailed characterization of chemistry and degradation mechanisms.
- Work with industrial partner to develop full-scale engine-catalyst systems to meet efficiency and emissions goals.

Approach

- Develop improved analytical techniques for characterizing combustion and catalyst chemistry.
- Conduct detailed evaluations of reaction order and contribution, as well as deactivation method effects.
- Perform system-level evaluations of effectiveness/efficiency of select engine-catalyst system parameters.

Accomplishments

- Applied spatially resolved capillary inlet mass spectrometer (SpaciMS) and phosphor thermography (PhosT) instruments for quantitative and minimally invasive in-operando intra-catalyst measurement of transient species and temperature distributions, respectively.
- Quantified network and sequence of reactions associated with lean NOx trap (LNT) regeneration via CO.
- Clarified relevance of the water-gas shift (WGS) reaction to LNT regeneration.

Future Directions

- Quantify select effects of deactivation mechanisms on the efficiency of reactions relevant to the CRADA objectives.
- Evaluate the timing, priority and significance of various detailed reactions involved in reactor chemistry relevant to the CRADA objectives.
- Investigate variations in reaction effectiveness with reaction parameters.
- Develop and apply diagnostics to optimize engine-catalyst system-evel parameters to enhance diesel efficiency and viability.

Introduction

Increasing expectations for efficiency, fuel economy, and low emissions from heavy-duty vehicles require corresponding improvements in system design. The realm of expectation is now sufficiently high as to require carefully integrated engine-catalyst-control systems working in precise concert. This level of design and control requires detailed knowledge of the combustion and catalyst chemistry; i.e., what reactants make the catalyst most efficient, what is the sequence and significance of

reactions throughout the system, and how can the engine/system be controlled to enhance catalyst efficiency? This CRADA project takes a parallel approach with highly controlled bench-scale and more final-product-indicative full-engine-scale research to address these issues.

Approach

The big-picture approach that has been used in this CRADA project is to combine the unique resources available at Cummins Inc. and Oak Ridge National Laboratory to improve the efficiency of the target diesel engine systems. The approach uses parallel bench-component and full-engine-scale investigations. The goal of such studies is to establish a more detailed understanding of the components and system operation, so that pathways to efficiency improvements and technology barriers can be identified. These technology limitations include analytical technique deficiencies that limit the detail with which the system can be characterized. As suggested by the project title, developing advanced measurement technology when necessary to improve characterization ability is also a central purpose of this project. Continual refinement of detailed system knowledge and the analytical techniques used to establish that knowledge enhances the team's ability to correspondingly improve the efficiency, fuel economy and emissions of the diesel engine system.

Results

To obtain a detailed understanding of LNT regeneration under practical, relevant conditions, a standard NOx storage/regeneration fast-cycling experiment was performed (details in Table 1). To facilitate deconvolution of the multiple potential CO reactions (CO+NO; CO+O_2; CO+H_2O), fast-cycling experiments were also performed without NO during storage, as well as in the absence of both NO and O_2 in the feed throughout the cycling experiment. The intra-catalyst gas composition and reaction temperature were analyzed at different axial locations with high temporal resolution via SpaciMS and PhosT, respectively. SpaciMS probes were placed in 0.75-in increments within the catalyst: catalyst inlet (0.0 in), ¼ position (0.75 in), ½ position (1.5 in), ¾ position (2.25 in) and catalyst outlet (3.0 in). PhosT probes were placed in 0.5-in increments: -0.5 in, 0.0 in, 0.5 in, 1.0 in, 1.5 in, 2.0 in, 2.5 in.

Table 1. Details of the Standard NOx Storage/ Regeneration Cycling Experiment

	Storage (lean)	Regeneration (rich)
Duration	56 s	4 s
Space velocity	30,000 h^{-1}	30,000 h^{-1}
NO	250 ppm	0 ppm
CO	0%	4%
O_2	8%	1%
H_2O	5%	5%
N_2	Balance	Balance

Nature and sequence of reactions occurring during LNT regeneration with CO reductant

The SpaciMS data demonstrated gas-phase O_2 depletion within the first ¼ of catalyst during regeneration (Figure 1). The PhosT measurements indicated that O_2 depletion was achieved even before the ¼ position (Figures 2 and 3). Indeed, if the temperature profile at the 0.0-in position of Figure 2 is compared with that of Figure 3, it is clear that the CO+O_2 reaction produced the large exotherm whose maximum coincided with regeneration termination and that this reaction did not produce significant exotherm beyond the 0.5-in position. This

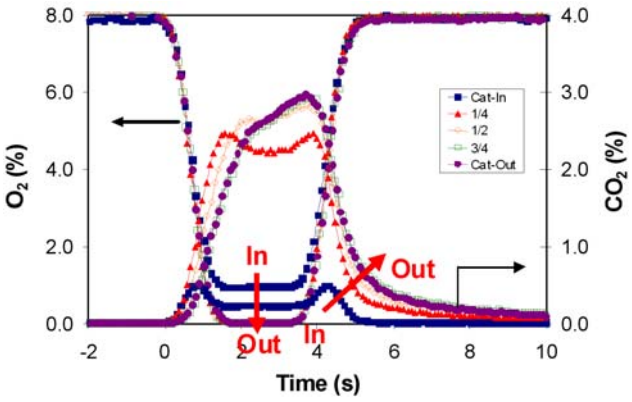

Figure 1. Transient, Spatially Resolved Intra-Catalyst O_2 and CO_2 Breakthrough Profiles Before, During, and After Regeneration

observation indicates that O_2 depletion was nearly complete at the 0.5-in (1/6-cat) position. The synchronous timing of the catalyst-face temperature maximum and regeneration termination is in accordance with O_2 depletion by CO over the entire regeneration period (Figure 1).

Logically, the smaller exotherm observed at early regeneration times in Figure 2 and missing in Figure 3 was due to the CO+NOx reaction. The axially extended nature of this exotherm is consistent with the axial distribution of stored NOx. The NOx-attributable exotherm existed only over early regeneration times (~ first 2 s), contrary to the CO+O_2 reaction exotherm (entire 4 s). Associating the PhosT and SpaciMS measurements, the temporal and spatial location of NOx release/reduction can be deduced. In fact, SpaciMS NOx profiles (Figure 4) alone indicate only the timing of total NOx slip; corresponding N_2, NO, NO_2, N_2O, and NH_3 data are necessary to determine the exact timing of NOx release/reduction. However, from the temporal coincidence of the NOx-attributable exotherm (Figure 2) and the NOx slip distributions (Figure 4), it is clear that SpaciMS NOx profiles indicate actual timing of NOx release/reduction for the case studied. Moreover, the spatial confinement of the NOx-attributable exotherm to within the 1.5-in position (Figure 2) is consistent with near-exclusive NOx storage within the first ½ (Figure 4). Fourier transform infrared (FTIR) was used for additional characterization of the dynamic catalyst-out species pool (Figure 5).

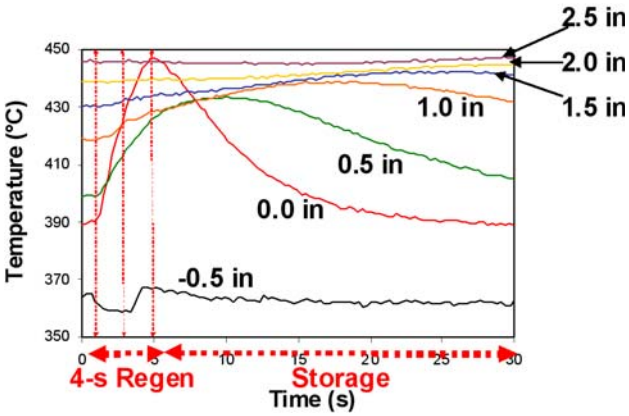

Figure 2. Transient, Spatially Resolved Intra-Catalyst Temperature Profiles with Both CO+NOx and CO+O_2 Reactions

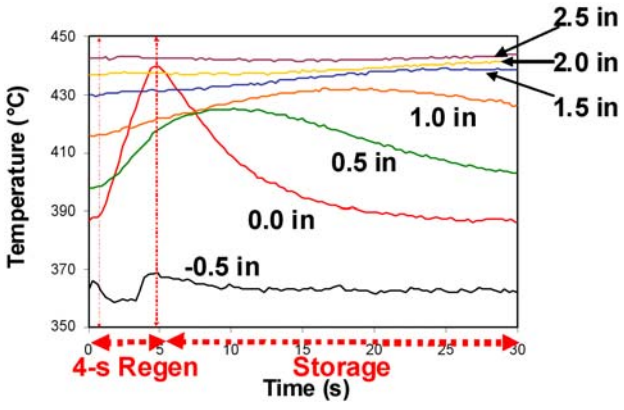

Figure 3. Transient, Spatially Resolved Intra-Catalyst Temperature Profiles with Only the CO+O_2 Reaction

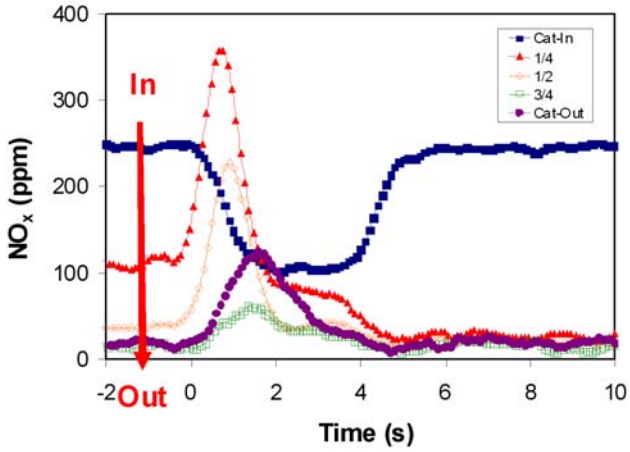

Figure 4. Transient, Spatially Resolved Intra-Catalyst NOx Breakthrough Profiles Before, During, and After Regeneration

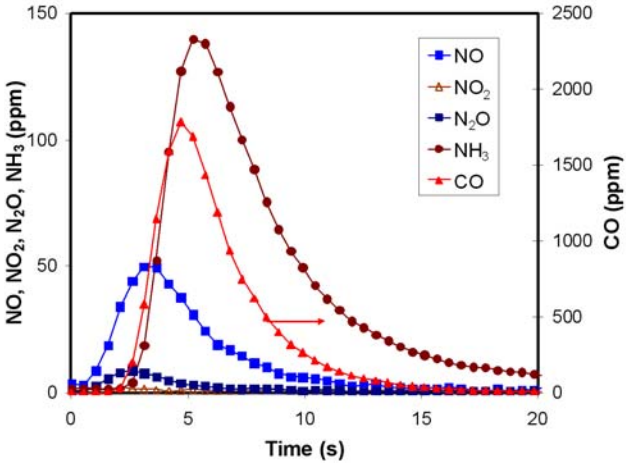

Figure 5. FTIR Analysis of Catalyst-Outlet Gas Composition

In summary, NOx release/reduction was highly efficient, and the "primary" NOx release/reduction was completed at early regeneration times inside the first ½ of catalyst. The term "primary" indicates that not all stored NOx was removed at early regeneration times. In fact, some portion of NOx was still being removed from the catalyst at late regeneration times, as indicated by late NH_3 generation (Figure 5). Although FTIR signal broadening makes exact sequencing of events difficult, it is clear that NH_3 appeared later than NO, N_2O and CO breakthrough. It appears that two distinct NOx release/reduction schemes were involved during regeneration, and we enumerate their respective features as follows:

- "Primary" release/reduction: occurred at early regeneration times; treated major portion of the NOx; small NO slip probably due to limited CO supply; produced N_2 as major reduction product.
- "Secondary" release/reduction: occurred after primary release/reduction; minor portion of the NOx; no NO slip; occurred in CO excess; produced NH_3 as major reduction product.

Further studies are necessary to understand the underlying mechanisms responsible for these two distinct NOx release/reduction features. For example, confirmation of the earlier N_2 formation compared to NH_3 would be required via direct N_2 measurement. On the other hand, more experimental data will be necessary to elucidate underlying mechanisms of NH_3 formation with pure CO as the reductant.

Impact of WGS reaction on LNT regeneration

The SpaciMS and PhosT instruments were used for in-operando characterization of the impact of the WGS reaction on LNT regeneration. The results are described in an archival publication [1], but are not included here due to space limitations.

Conclusions

Two ORNL-developed minimally invasive diagnostics, SpaciMS and PhosT, were applied to studies of LNT chemistry under practical and relevant fast-cycling conditions. Dynamic species and temperature distributions throughout an operating LNT device were resolved, leading to new insights into LNT regeneration with a CO reductant (network and sequence of reactions; reaction exotherms and heat transfer). Findings include the following:

- Gas-phase O_2 reacts with CO very efficiently over the entire 4-s regeneration period. Only a small front portion of the monolith is necessary for complete O_2 depletion.
- Depletion of gas-phase O_2 results in a large exotherm at the monolith front end which dissipates slowly over time. This slow heat dissipation significantly raises the subsequent storage-phase temperature.
- Primary NOx release/reduction is vigorous and occurs at early regeneration times with small NO and N_2O slip.
- Secondary NOx release/reduction takes place at later regeneration times with NH_3 as the main product.
- The exotherm due to the primary NOx-CO reaction is smaller than that due to the O_2-CO reaction, but it is produced over a greater front portion of the catalyst due to axially distributed NOx storage.
- The studied catalyst is active in the WGS reaction. CO reacts first with surface H_2O adsorbed during the preceding storage before consuming gas-phase H_2O. However, it appears that the WGS reaction is not active during O_2 depletion and primary NOx release/reduction due to the relatively slow rate of the WGS reaction relative to competing CO reactions. Apparently, suppressed WGS reaction is accompanied by the displacement of "pre-adsorbed" surface H_2O by CO_2 produced by O_2 depletion and the primary NOx-release/reduction reactions.
- Apparent temperature rise due to the WGS reaction is insignificant.
- Further work is necessary to assess the impact of the WGS reaction on secondary NOx release/reduction.

The detailed chemistry provided in this effort is not easily obtainable via conventional "catalyst-outlet-only" analytical tools. This type of intra-catalyst data will be useful for improved LNT formulations, predictive kinetic models development and validation, fuel-efficient systems and control strategy development.

FY 2005 Publications/Presentations

1. Jae-Soon Choi, William P. Partridge, William S. Epling, Neal W. Currier, Thomas M. Yonushonis, "Intra-channel evolution of carbon monoxide and its implication on the regeneration of a monolithic $Pt/K/Al_2O_3$ NO_x storage-reduction catalyst", *Catalysis Today*, accepted.
2. Jae-Soon Choi, William P. Partridge, and C. Stuart Daw, "Spatially-resolved *in situ* measurements of transient species breakthrough during cyclic, low-temperature regeneration of a monolithic $Pt/K/Al_2O_3$ NO_x storage-reduction catalyst", *Applied Catalysis A* **293**, 24-40 (2005).
3. Jae-Soon Choi, William P. Partridge, William S. Epling, Neal W. Currier, and Thomas M. Yonushonis, "Intra-channel evolution of carbon monoxide and its implication on the regeneration of a monolithic $Pt/K/Al_2O_3$ NO_x storage-reduction catalyst", Southeastern Catalysis Society Fall Symposium, Asheville, North Carolina, September 25-26, 2005.
4. Jae-Soon Choi, William P. Partridge, William S. Epling, Neal W. Currier, and Thomas M. Yonushonis, "Intra-channel evolution of carbon monoxide and its implication on the regeneration of monolithic NO_x storage-reduction catalyst based on $Pt/K/Al_2O_3$", 19th North American Catalysis Society Meeting, Philadelphia, Pennsylvania, May 22-27, 2005.
5. James E. Parks, Todd J. Toops, William P. Partridge, Jae-Soon Choi, Brian H. West, Shean P. Huff, and C. Stuart Daw, "Overview: NO_x adsorber catalysis for diesel emission control", 19th North American Catalysis Society Meeting, Philadelphia, Pennsylvania, 2005.
6. Jae-Soon Choi, William Partridge, and C. Stuart Daw, "Spatially-resolved in situ measurements of transient species breakthrough during low-temperature regeneration of a $Pt/K/Al_2O_3$ lean NO_x trap", 8th DOE Crosscut Workshop on Lean Emissions Reduction Simulation, Dearborn, Michigan, May 17-19, 2005.
7. William P. Partridge, Jae-Soon Choi, and Steve Allison, "Minimally invasive diagnostics for intra-reactor measurements of species and temperature", 51th International Instrumentation Symposium, Knoxville, Tennessee, May 9-12, 2005.

II.B.10 Off-Highway Engine Emission Control with High System Efficiency (CRADA with John Deere Product Engineering Center)

Michael D. Kass (Primary Contact), Norberto Domingo, John M. E. Storey
Oak Ridge National Laboratory
NTRC
2360 Cherahala Blvd.
Knoxville, TN 37932

DOE Technology Development Manager: John Fairbanks

Objectives

- Evaluate the potential of NOx-reducing aftertreatment technologies to achieve interim Tier 4 NOx emission levels for off-highway heavy-duty diesel engines. The initial focus is to utilize a urea-based selective catalytic reduction (SCR) system to achieve brake-specific NOx levels of 2 g/kWh over the ISO 8178 off-highway test cycle.
- Optimize key injection parameters to achieve improvements in fuel efficiency while meeting the 2011 Tier 4 emission levels for NOx. The initial target value for brake-specific fuel consumption is 195 g/kWh.

Approach

- Install and set up a urea-SCR system in the exhaust system of a heavy-duty off-highway engine. The system consists of an oxidation catalyst, Bosch urea injector and dosing unit, and a Johnson-Matthey urea-SCR catalyst.
- Evaluate the performance of the urea-SCR system to reduce NOx emissions for six modes of the ISO 8178 off-highway test cycle. Examine the slip of ammonia from the SCR catalyst during urea injection.
- Analyze the performance of the urea-SCR system to identify areas of further improvement.
- Evaluate the influence of rail pressure to lower particulate matter (PM) emissions for each of the eight modes of the ISO 8178 off-highway test cycle.

Accomplishments

- The gravimetric PM emissions were reduced 75% by raising the rail pressure for the ISO 8178 test cycle. The PM emissions were further lowered an additional 50% when ultra-low sulfur diesel (ULSD) fuel was used in combination with the high rail pressure. Therefore, the Tier 4 PM milestone (0.02 gPM/kWh) was achieved when operating the engine at high rail pressure and utilizing ULSD fuel.
- Although the high rail pressure increased the NOx emissions dramatically, the utilization of urea-SCR improved the baseline NOx emissions by 43% over the ISO 8178 test cycle.

Future Directions

- Conduct evaluation and analysis of PM emissions while metering urea for NOx conversion.
- Conduct detailed evaluations (combined engine and bench studies) on the urea decomposition kinetics for different engine operating conditions.
- Evaluate the influence of alternative fuels on engine efficiency and the performance of the urea-SCR system.
- Evaluate the influence of alternative fuels on PM formation under conditions of high rail pressure.

Introduction

Tier 3 federal standards for new off-highway diesel engines require that NOx and PM levels be regulated to 4 g/kWh and 0.2 g/kWh, respectively, for engines between 130 and 560 kW. The phase-in period for Tier 3 compliance is set to begin in 2006 and to be completed by 2008. Urea-SCR has been shown to effectively reduce NOx emissions for on-highway and stationary applications, but needs to be thoroughly evaluated for off-highway engines since both engine design and operating conditions are different. The utilization of advanced injection systems and controls is to be evaluated for improvements in both PM emissions and brake-specific fuel consumption (BSFC). This project seeks to develop and evaluate emission control methodologies with the goal of identifying pathways to meet interim Tier 4 and retrofit solutions.

Approach

The principal activity for FY 2005 was to evaluate a strategy to reduce PM and NOx emissions using a combination of engine controls and urea-selective catalytic reduction. The approach was to reduce PM emissions to Tier 4 levels by utilizing advanced injection strategies, especially increasing the rail pressure. To overcome the high NOx emissions associated with higher rail pressure, a urea-SCR system was incorporated into the exhaust system and evaluated to determine the potential of this approach to lower NOx emissions to interim Tier 4 levels. A urea-SCR catalyst was added to the test cell (an earlier version had failed) and evaluated according to the ISO 8178 C1 test cycle. Data were collected for a range of urea delivery rates, up to and exceeding the stoichiometric rate of application. Ammonia slip and NO_2 were measured for each operating mode.

In order to better elucidate the formation of PM in the exhaust system, which contained a diesel oxidation catalyst (DOC) and a urea-SCR catalyst, the particulate matter was collected and analyzed as a function of location within the exhaust for a No. 2 certification fuel (containing approximately 350 ppm sulfur) and an ULSD fuel. A third activity for this fiscal year was to evaluate a proprietary injection strategy to produce a rich exhaust gas environment.

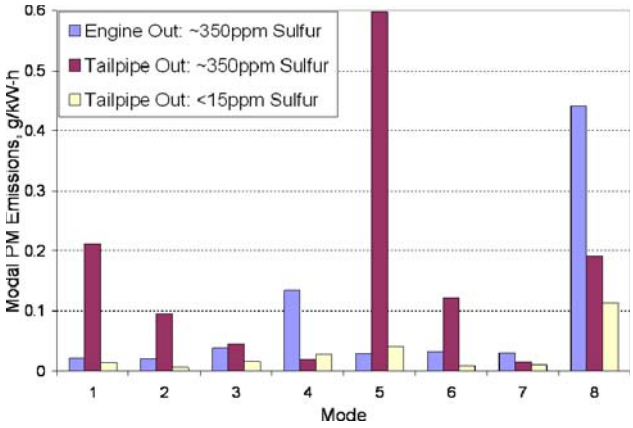

Figure 1. Modal PM Emissions as a Function of Fuel Sulfur Level and Exhaust Sample Point.

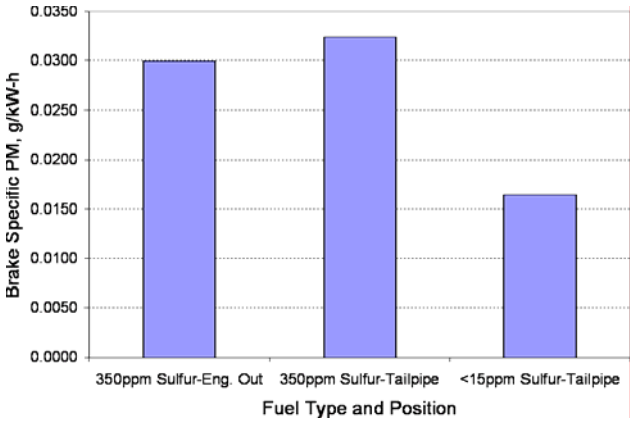

Figure 2. Brake-Specific PM Emissions, Based on the ISO 8178 8-Mode Test Cycle, as a Function of Fuel Sulfur Level and Exhaust Sample Point.

Results

Particulate emissions were collected and analyzed using a No. 2 certification fuel (~350 ppm sulfur) and an ULSD fuel (<15 ppm sulfur). While running on No. 2 certification fuel, particulate emissions were collected upstream of the DOC and downstream of the urea-SCR catalyst. For the ULSD fuel, particulate emissions were collected downstream of the urea-SCR catalysts only. The results are shown for each mode in Figure 1 and as brake-specific values in Figure 2. As shown in these figures, the particulate mass was influenced by the fuel type, and for No. 2 certification fuel, the engine-out particulate mass was increased by 8% after passing over the DOC and urea-SCR catalyst. This is caused by the oxidation of gaseous SO_2 into sulfates which contribute to PM mass and formation. The

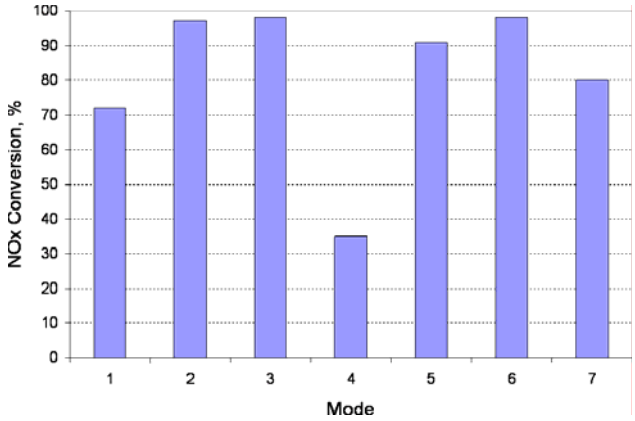

Figure 3. Maximum NOx Conversion Efficiency for Each Operating Mode Utilizing Urea-SCR

tailpipe particulate emissions were lower for the ULSD fuel, and in fact were within the Tier 4 limit of 0.02 g/kWh.

The NOx conversion efficiencies achieved using the urea-SCR system are shown in Figure 3. The NOx conversion efficiency was over 90% for modes 2, 3, 5, and 6. For these modes, the catalyst temperature was within the optimum conversion temperature range. Interestingly, in spite of being within the optimum temperature window, the maximum conversion efficiency for mode 1 was only 70%. Since the space velocity at this mode is also the highest, it is probable that the catalyst size was too small to enable higher conversion efficiency.

When the rail pressure was increased to the maximum setting, the NOx emissions increased from a baseline value of 5.25 g/kWh to over 14 g/kWh. The urea-SCR system was able to reduce this value to 2.3 g/kWh, which is very close to the interim Tier 4 level of 2.0 g/kWh. It is quite likely that a more appropriately sized catalyst would enable high NOx conversion for mode 1, thereby reducing the NOx emissions to within interim Tier 4 limits. Ammonia slip was found to be dependent on space velocity; it was detected for the high speed points (2400 rpm), but not for the low speed conditions (1400 rpm). Also, very low levels of N_2O were formed during the evaluation.

Conclusions

- Met Tier 3 NOx emission levels utilizing urea-SCR. May be able to obtain Tier 4 interim levels with a larger catalyst. Ammonia slip was only detected at high space velocity conditions. No significant formation of N_2O was observed.
- Achieved the PM target utilizing high rail pressures in combination with ultra-low sulfur diesel fuel. When running the engine using No. 2 certification fuel (~350 ppm sulfur content), sulfates were formed in the DOC which added to particulate mass.